

## REVIEW

# Regulated Necrosis in Atherosclerosis

Pauline Puylaert<sup>1</sup>, Michelle Zurek<sup>1</sup>, Katey J. Rayner<sup>1</sup>, Guido R.Y. De Meyer<sup>1</sup>, Wim Martinet<sup>1</sup>

**ABSTRACT:** During atherosclerosis, lipid-rich plaques are formed in large- and medium-sized arteries, which can reduce blood flow to tissues. This situation becomes particularly precarious when a plaque develops an unstable phenotype and becomes prone to rupture. Despite advances in identifying and treating vulnerable plaques, the mortality rate and disability caused by such lesions remains the number one health threat in developed countries. Vulnerable, unstable plaques are characterized by a large necrotic core, implying a prominent role for necrotic cell death in atherosclerosis and plaque destabilization. Necrosis can occur accidentally or can be induced by tightly regulated pathways. Over the past decades, different forms of regulated necrosis, including necroptosis, ferroptosis, pyroptosis, and secondary necrosis, have been identified, and these may play an important role during atherogenesis. In this review, we describe several forms of necrosis that may occur in atherosclerosis and how pharmacological modulation of these pathways can stabilize vulnerable plaques. Moreover, some challenges of targeting necrosis in atherosclerosis such as the presence of multiple death-inducing stimuli in plaques and extensive cross-talk between necrosis pathways are discussed. A better understanding of the role of (regulated) necrosis in atherosclerosis and the mechanisms contributing to plaque destabilization may open doors to novel pharmacological strategies and will enable clinicians to tackle the residual cardiovascular risk that remains in many atherosclerosis patients.

**GRAPHIC ABSTRACT:** A [graphic abstract](#) is available for this article.

**Key Words:** atherosclerosis ■ ferroptosis ■ necroptosis ■ necrosis ■ pyroptosis

Atherosclerosis is a progressive inflammatory disease of large- and medium-sized muscular arteries and typically leads to the formation of plaques, which can reduce blood flow to tissues. When a plaque develops an unstable phenotype, it is prone to rupture, which can lead to myocardial infarction, stroke, and sudden death. The global aim in the treatment of atherosclerosis is the prevention of cardiovascular complications.<sup>1</sup> Lifestyle changes, including dietary lipid lowering, regular physical activity, smoke cessation, and blood pressure control, are necessary measures in the prevention of the disease. If lifestyle changes are not sufficient, treatment with medications, such as those that lower circulating lipids, is recommended. However, despite tremendous advances in identifying and treating vulnerable plaques, the mortality rate and disability caused by such lesions still remains the number one health threat in developed countries. Statins and PCSK (proprotein convertase subtilisin/kexin type)-9 inhibitors reduce LDL (low-density lipoprotein)-cholesterol to low levels but do not eliminate residual cardiovascular risk as a result of other atherogenic lipoproteins or pathways for atherosclerotic

cardiovascular disease, including inflammation, that are independent of LDL-cholesterol.<sup>2</sup> This highlights the need for additional therapeutic strategies to prevent atherosclerotic plaque formation and rupture. Because cell death is a prominent feature of advanced atherosclerotic plaques, with a major impact on atherogenesis and plaque destabilization,<sup>3</sup> pharmacological modulation of cell death in atherosclerosis represents a promising therapeutic approach. Indeed, plaque cells may undergo diverse types of death of which apoptosis is the best characterized. However, electron microscopic examination of human plaques showed that the vast majority of disintegrating macrophages and vascular smooth muscle cells have an ultrastructure typical of necrosis (30±18% necrotic versus 1±2% apoptotic cells).<sup>4,5</sup> This finding suggests that although cell death by apoptosis clearly occurs in advanced human plaques, cells that accumulate in vulnerable plaques die by necrosis.

Necrotic cell death is characterized by an increased cell volume (oncosis), organelle swelling and chromatin condensation, which eventually culminates in plasma membrane rupture and the release of intracellular compounds.<sup>6</sup>

Correspondence to: Wim Martinet, PhD, Laboratory of Physiopharmacology, University of Antwerp, Universiteitsplein 1, B-2610 Antwerp, Belgium. Email [wim.martinet@uantwerpen.be](mailto:wim.martinet@uantwerpen.be)

For Sources of Funding and Disclosures, see page 1301.

© 2022 American Heart Association, Inc.

*Arterioscler Thromb Vasc Biol* is available at [www.ahajournals.org/journal/atvb](http://www.ahajournals.org/journal/atvb)

## Nonstandard Abbreviations and Acronyms

<b>ACSL-4</b>	Acyl-CoA synthetase long chain family member 4
<b>ADME</b>	absorption, distribution, metabolism and excretion
<b>AP</b>	activator protein
<b>ASC</b>	apoptosis-associated speck-like protein containing a caspase recruitment domain
<b>CANTOS</b>	Canakinumab Anti-inflammatory Thrombosis Outcome Study
<b>CARD</b>	caspase recruitment domain
<b>ciAP</b>	cellular inhibitors of apoptosis
<b>DAMP</b>	damage-associated molecular pattern
<b>DNL</b>	Denali Therapeutics
<b>ERK</b>	extracellular signal-regulated kinase
<b>FADD</b>	fas-associated death domain
<b>FasL</b>	first apoptotic signal ligand
<b>FSP</b>	ferroptosis suppressor protein
<b>GFH</b>	Genfleet Therapeutics
<b>GPX-4</b>	glutathione peroxidase 4
<b>GSDMD</b>	gasdermin D
<b>GSDME</b>	gasdermin E
<b>GSK</b>	GlaxoSmithKline
<b>GSR</b>	glutathion-disulfide reductase
<b>GSS</b>	glutathion synthetase
<b>GSSG</b>	glutathion disulfide
<b>HMGB-1</b>	high-mobility group box 1
<b>HMOX-1</b>	heme oxygenase 1
<b>IKK</b>	IkB kinase
<b>IL</b>	interleukin
<b>iNOS</b>	inducible nitric oxide synthase
<b>JNK</b>	c-Jun N-terminal kinase
<b>LDL</b>	low-density lipoprotein
<b>LOX</b>	lipoxygenase
<b>LPCAT</b>	lysophosphatidyl acyltransferase
<b>MAPK</b>	mitogen-activated protein kinase
<b>MLKL</b>	mixed lineage kinase domain-like protein
<b>Nec-1s</b>	necrostatin-1s
<b>NEMO</b>	NF-κB essential modulator
<b>NF-κB</b>	nuclear factor-κB
<b>NLRP-3</b>	nucleotide-binding oligomerization domain-like, leucine-rich repeat, and pyrin domain-containing receptor 3
<b>Nrf-2</b>	nuclear factor erythroid 2-related factor 2
<b>NT-GSDMD</b>	N-terminal cleavage product of gasdermin D
<b>oxLDL</b>	oxidized low-density lipoprotein
<b>PAMP</b>	pathogen-associated molecular pattern

<b>PCSK-9</b>	proprotein convertase subtilisin/kexin type 9
<b>PRR</b>	pattern-recognition receptor
<b>PTGS2</b>	prostaglandin-endoperoxide synthase 2
<b>PYD</b>	pyrin domain
<b>RAGE</b>	receptor for advanced glycation endproducts
<b>RHIM</b>	RIP homotypic interaction motif
<b>RIPK</b>	receptor-interacting protein kinase
<b>ROS</b>	reactive oxygen species
<b>RSL3</b>	Ras selective lethal 3
<b>TAB</b>	TGF-β activated kinase 1 (MAP3K7) binding protein
<b>TAK</b>	transforming growth factor β-activated kinase
<b>TLR</b>	Toll-like receptor
<b>TNF-α</b>	tumor necrosis factor α
<b>TRADD</b>	TNF receptor type 1-associated death domain protein
<b>TRAIL</b>	TNF-related apoptosis inducing ligand
<b>TUNEL</b>	terminal deoxynucleotidyl transferase dUTP nick-end labeling
<b>zVAD-fmk</b>	carbobenzyloxy-valyl-alanyl-aspartyl-[O-methyl]-fluoromethylketone

## Highlights

- The majority of dying cells in advanced human atherosclerotic plaques undergo necrosis.
- Necrotic death stimulates atherogenesis and plaque instability through induction of inflammation and enlargement of a central necrotic core.
- Apart from accidental necrosis, regulated (programmed) necrosis is a major contributor to necrotic core formation and plaque destabilization.
- Cells in atherosclerotic plaques may undergo different types of regulated necrosis, including necroptosis, pyroptosis, and ferroptosis.
- Regulated necrosis can be efficiently blocked with potent and selective inhibitors targeting key regulators in the necrosis pathway.

Accumulation of necrotic cells and their contents triggers the formation and enlargement of a central necrotic core (Figure 1), which is a hypocellular region containing lipids and cellular debris.<sup>7</sup> The majority (80%) of necrotic cores in advanced human atherosclerotic plaques are larger than 1 mm<sup>2</sup>, which compromises >10% of the lesion area.<sup>8</sup> However, in 65% of plaque ruptures, the necrotic core occupies >25% of the plaque area,<sup>8</sup> suggesting that it plays a pivotal role in unstable atherosclerotic plaques. Virtually all advanced human plaques have areas of necrosis.<sup>9,10</sup>

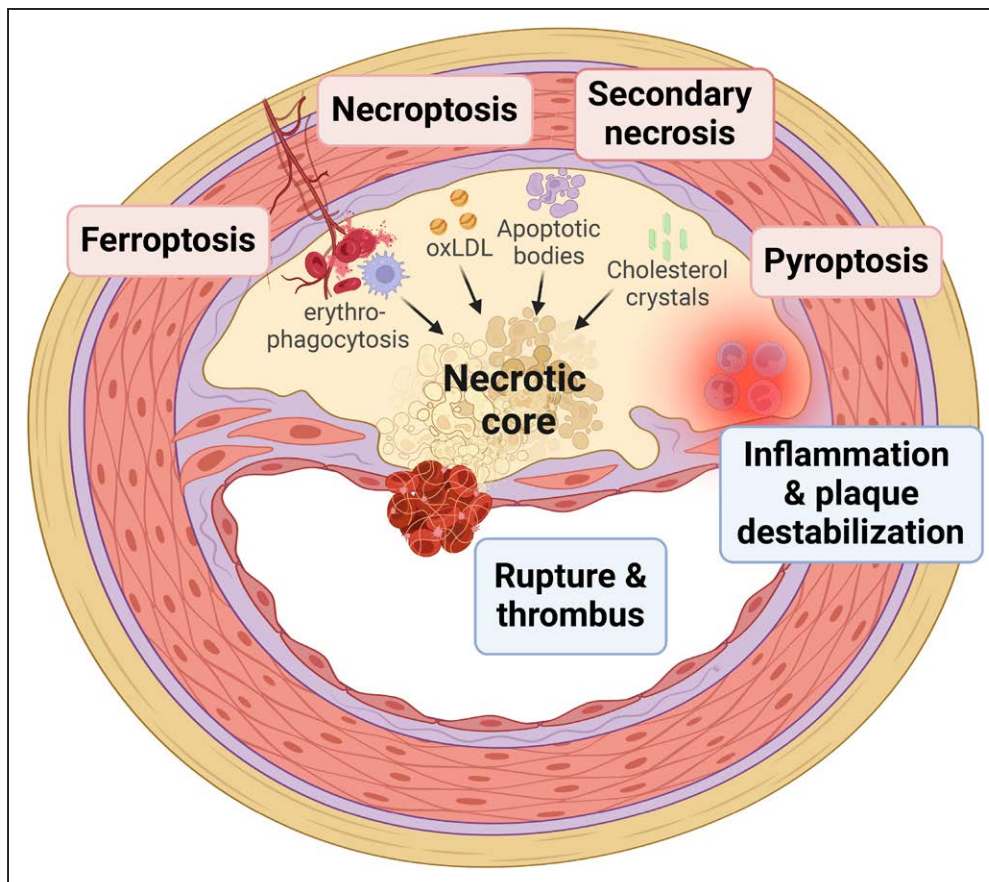


**Figure 1. Overview of generally known regulated necrosis triggers in the atherosclerotic plaque and their impact on plaque progression and destabilization.**

In atherosclerosis, necrosis can occur accidentally or be induced by tightly regulated pathways, eventually leading to the development of a large hypocellular region containing remnants of dead cells known as the necrotic core. During plaque progression, the hypoxic environment inside the plaque can induce neovascularization. Since intraplaque neovessels are commonly leaky, inflammatory blood cells are recruited, and intraplaque hemorrhage occurs. Macrophages surrounding intraplaque hemorrhage phagocytose erythrocytes (erythrophagocytosis), leading to HMOX-1 (heme oxygenase 1) activation, high intracellular levels of heme and iron, and consequently ferroptosis. Moreover, oxLDL (oxidized low-density lipoprotein) increases reactive oxygen species (ROS)-mediated RIPK (receptor-interacting protein kinase)-3 and MLKL (mixed lineage kinase domain-like protein) gene expression in macrophages, triggering necroptosis. As apoptotic bodies accumulate in advanced plaques, efferocytosis falls short and gets impaired, resulting in secondary necrosis. Cholesterol crystals in atherosclerotic plaques activate NLRP (nucleotide-binding oligomerization domain-like, leucine-rich repeat, and pyrin domain-containing receptor)-3 inflammasomes through lysosomal rupture leading to the induction of pyroptosis. Different forms of regulated necrosis contribute to expansion of the necrotic core which induces inflammation, plaque destabilization, fibrous cap rupture, and thrombus formation. Image created with Biorender.

Noteworthy is that both early and late stages of necrotic cores are recognized. Areas of early necrotic core formation typically show free cholesterol with mostly intact macrophages and extracellular matrix made up of proteoglycans. In contrast, late stage necrotic cores show numerous cholesterol clefts, cellular debris, and absence of extracellular matrix.<sup>10</sup> It should be noted that the core region is not only critical for plaque stability but also for thrombogenicity. The necrotic core contains high concentrations of tissue factor,<sup>11</sup> suggesting that plaque cells undergoing necrosis mediate thrombus formation after plaque rupture.

Apart from the formation and enlargement of a central necrotic core, necrotic macrophages in advanced plaques are a source of proinflammatory cytokines and damage-associated molecular patterns (DAMPs).<sup>12</sup> The release of DAMPs promotes inflammation in the plaque,

thereby contributing to plaque instability. HMGB-1 (High-mobility group box 1) protein is one of the best studied DAMPs in atherosclerosis and is abundantly produced by plaque macrophages.<sup>13</sup> Once released in the extracellular space, HMGB-1 interacts with different receptors including RAGEs (receptor for advanced glycation end-products). Binding of HMGB-1 triggers the transcription of proinflammatory cytokines in an NF- $\kappa$ B (nuclear factor- $\kappa$ B) dependent manner, thereby promoting further plaque development.<sup>14</sup> Experimental evidence has shown that HMGB-1 expression increases during atherogenesis.<sup>13</sup> Neutralization of HMGB-1 in ApoE<sup>-/-</sup> mice reduces plaque area through inhibition of immune cell accumulation and macrophage migration.<sup>15</sup> Interestingly, increasing experimental evidence suggests that statins attenuate plaque formation partly by reducing the expression of

HMGB-1 and RAGE.<sup>16–18</sup> The release of HMGB-1 and other DAMPs or proinflammatory mediators is not only characteristic of necrosis but also occurs in senescent cells. Indeed, senescence is a dynamic process resulting in cell cycle arrest and accompanied by a proinflammatory senescence-associated secretory phenotype, which is proatherogenic.<sup>19,20</sup> Consequently, senescent cells are proinflammatory and undergo metabolic changes, but they remain viable. This contrasts with apoptotic and necrotic cells which lose viability irreversibly and are destined to disappear, either silently (apoptosis) or leaving a proinflammatory footprint behind (necrosis). Different intraplaque cell types, such as endothelial cells, vascular smooth muscle cells, macrophages, and T cells, can undergo senescence or cell death, but the total number of senescent versus dying cells in atherosclerotic plaques remains elusive and is complicated by their shared characteristics (eg, increased cell volume, DNA breaks, release of proinflammatory cytokines, and DAMPs) and interplay.<sup>20,21</sup>

Necrosis in atherosclerotic plaques can occur accidentally (eg, when cholesterol crystals puncture the plasma membrane) or can be induced following activation of tightly regulated pathways (Figure 1). In this review, we describe different types of regulated necrosis that may occur in atherosclerosis and how pharmacological targeting of these types of death can stabilize vulnerable plaques and contribute to the beneficial effects of currently applied plaque stabilizing therapies.

## NECROPTOSIS

Research in the field of necrotic cell death was drastically changed by the discovery of small molecules, termed necrostatins, which inhibit RIPK (receptor-interacting protein kinase)-1-induced necroptosis in TNF (tumor necrosis factor)- $\alpha$ -treated cells.<sup>22,23</sup> This discovery led to the characterization of downstream necroptosis mediators, namely RIPK-3 and MLKL (mixed lineage kinase domain-like protein; Figure 2).<sup>24–27</sup> In addition to TNF- $\alpha$ , other necroptosis triggers have been identified, including TRAIL (TNF-related apoptosis inducing ligand), FasL (first apoptotic signal ligand), interferons, TLR (Toll-like receptor) ligands, and virus-activated pathways.<sup>28</sup>

### Activation of the RIPK-1/RIPK-3/MLKL-Axis After TNF- $\alpha$ Stimulation

The response of cells to TNF- $\alpha$  is complex and primarily depends on the ubiquitination and phosphorylation profile of RIPK-1 (Figure 2).<sup>29</sup> Upon TNF- $\alpha$  binding, TRADD (TNF receptor type 1-associated death domain protein) and RIPK-1 are recruited to form a membrane-bound complex I. Subsequently, the default response to TNF- $\alpha$  signaling is ubiquitination of RIPK-1 by cIAP (cellular inhibitors of apoptosis)-1/2 and linear ubiquitin chain assembly

complexes followed by the activation of prosurvival pathways including NF- $\kappa$ B and MAPK (mitogen-activated protein kinase) signaling. In this case, ubiquitinated RIPK-1 merely serves as a scaffold for binding and activation of mediators of NF- $\kappa$ B and MAPK pathways. In contrast, when protein synthesis of endogenous apoptosis inhibitors is blocked, for example by cycloheximide, or when ubiquitination and NF- $\kappa$ B activation are reduced, RIPK-1 switches from a prosurvival scaffold to a cytosolic prodeath protein.<sup>30,31</sup> In that case, necroptosis and apoptosis pathways compete and the presence and catalytic activity of caspase-8 plays a decisive role. Indeed, necroptosis proteins RIPK-1 and RIPK-3 are activated when caspase-8 is inhibited, combined with reduced RIPK-1 ubiquitination and NF- $\kappa$ B signaling.<sup>30</sup> Inhibition of caspase-8 can be obtained pharmacologically with the pan-caspase inhibitor zVAD-fmk (carbobenzoxy-valyl-alanyl-aspartyl-[O-methyl]-fluoromethylketone). However, the molecular mechanisms underlying caspase-8 inhibition and RIPK-1/RIPK-3 activation in atherosclerotic plaques are unclear. Most likely, oxidation or iNOS (inducible nitric oxide synthase)-driven S-nitrosylation (ie, inactivation) of a critical thiol-residue in the active site of caspase-8, in combination with proapoptotic signaling, triggers necroptosis induction. Macrophages overexpressing iNOS frequently surround the necrotic core of human plaques, which favors this hypothesis.<sup>32</sup> Interestingly, genetic deletion or deficiency of caspase-8 (or its adaptor TRADD) is associated with embryonic lethality in mice, which is attributed to necroptosis because deletion of RIPK-3 or MLKL rescues these mice. Lethality is mainly caused by defects in vascular development, underlining the importance of these pathways in cardiovascular disease.<sup>33</sup> Deletion of MLKL in caspase-8 deficient mice still causes perinatal lethality meaning that necroptosis-independent cell death is induced upon caspase-8 inhibition in later stages of embryonic development. Of note, this phenotype is rescued by deletion of ASC (apoptosis inhibitor speck-like protein) or caspase-1, both part of the pyroptosis machinery (vide infra), demonstrating that pyroptosis is induced when apoptosis and necroptosis are inhibited. Indeed, caspase-8 represents a molecular switch between apoptosis, necroptosis, and pyroptosis.<sup>33</sup>

Once activated, RIPK-1 undergoes autophosphorylation and interacts with RIPK-3 through a RHIM (RIP homotypic interaction motif) which results in RIPK-3 oligomerization and the formation of a necroptotic complex called the necrosome.<sup>34,35</sup> In the necrosome, RIPK-3 is activated resulting in a series of autophosphorylations and recruitment and phosphorylation of MLKL via its pseudokinase domain. As the name implies, the pseudokinase domain of MLKL topologically resembles a protein kinase domain but has no catalytic activity whatsoever and serves merely as an interaction domain with RIPK-3.<sup>34</sup> Finally, RIPK-3-induced phosphorylation of MLKL triggers its oligomerization. Phosphorylated MLKL oligomers associate with phospholipids in the plasma membrane, which

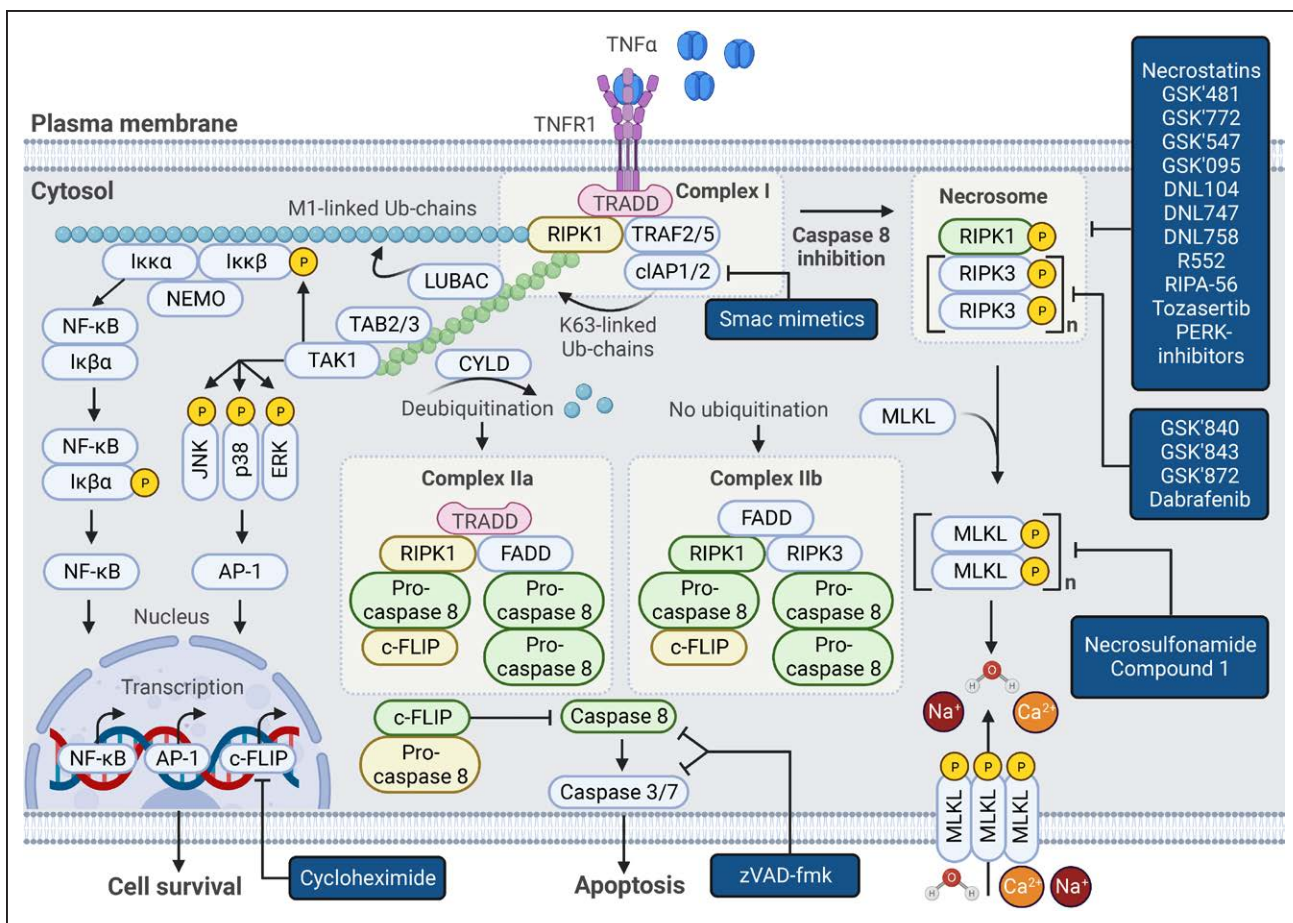


**Figure 2. Overview of TNF (tumor necrosis factor)-α-induced apoptosis and necroptosis pathways and potential targets for pharmacological inhibition.**

As TNF-α binds to trimeric TNFR (tumor necrosis factor receptor)-1, recruitment of tumor TRADD (TNFR1-associated death domain), and RIPK (receptor-interacting protein kinase)-1 is initiated. Consequently, TRAF (TNFR-associated factor)-2, TRAF-5, cIAP (cellular inhibitor of apoptosis protein)-1, and cIAP2 are recruited to TRADD, thereby forming complex I. cIAP-1/2 subsequently ubiquitinates RIPK-1 with K63-linked ubiquitin chains, allowing the recruitment of linear ubiquitin chain assembly complexes (LUBACs). Thereupon, LUBAC generates M1-linked ubiquitin chains, which then are added to RIPK-1. Subsequently, M1- and K63-ubiquitin chains act as a scaffold for the recruitment of IKK (IκB kinase)-α/IKK-β/NEMO (NF-κB essential modulator) and TAB (TGF-β-activated kinase 1-binding protein)-2/TAB-3/TAK (transforming growth factor β-activated kinase)-1, respectively. Next, TAK-1 phosphorylates IKK-β and the downstream MAPKs (mitogen-activated protein kinases) JNK (c-Jun N-terminal kinase), p38, and ERK (extracellular signal-regulated kinase), which activate transcription factor AP (activator protein)-1. Phosphorylated IKK-β activates IκBα resulting in the release of NF-κB (nuclear factor-κB). Subsequently, NF-κB translocates to the nucleus, resulting in the transcriptional upregulation of prosurvival genes. When cIAP-1/2 is depleted by smac mimetic-induced degradation or genetic ablation, RIPK-1 ubiquitination and NF-κB signaling are decreased. Simultaneous RIPK-1 deubiquitination by CYLD (cylindromatosis) protein will result in the release of RIPK-1 from complex I. Subsequently, RIPK-1 engages with FADD (fas-associated death domain), leading to the recruitment of procaspase-8 and c-FLIP (cellular FLICE-like protein long isoform) heterodimer and procaspase-8 homodimer, together forming complex IIa. Procaspase-8 and c-FLIP heterodimer inhibit the activation of caspase-8, thereby stimulating cell survival. In contrast, procaspase-8 homodimer generates active caspase-8, which in turn activates caspases-3 and -7 to induce apoptotic cell death. Whenever RIPK-1 is not ubiquitinated and transcription of apoptosis inhibitors is disrupted (eg, by cycloheximide), complex IIb, consisting of RIPK-1, RIPK-3, procaspase-8, and c-FLIP, will be formed. In contrast to complex IIa, the kinase activity of RIPK-1 is crucial for the induction of apoptosis via complex IIb. Pharmacological inhibition of apoptotic cell death can be achieved by pan-caspase inhibitors such as zVAD-fmk. When caspase-8 is inhibited, activation of RIPK-1 will not result in RIPK-1-kinase dependent apoptosis but will initiate the necroptosis pathway. In the cytosol, RIPK-1 binds to RIPK-3, resulting in a series of autophosphorylation and transphosphorylations of RIPK-1 and RIPK-3. Phosphorylated RIPK-3 consequently recruits and phosphorylates MLKL (mixed lineage kinase domain-like protein) leading to MLKL oligomerization. MLKL oligomers migrate to the plasma membrane where they induce necroptotic cell death by membrane permeabilization and deregulation of calcium and sodium channels. The activation state (green = active and yellow = inactive) of RIPK-1, caspase-8, and c-FLIP plays a decisive role in the cell's fate. Pharmacological inhibition of necroptosis is achieved with inhibitors of RIPK-1 kinase activity, RIPK-3, or MLKL. DNL indicates Denali Therapeutics; GFH, Genfleet Therapeutics; GSK, GlaxoSmithKline; and zVAD-fmk, carbobenzoxy-valyl-alanyl-aspartyl-[O-methyl]-fluoromethylketone. Image created with Biorender.

Downloaded from <http://ahajournals.org> by on November 9, 2022

causes plasma membrane permeabilization, release of DAMPs and eventually necroptotic cell death.<sup>27,36</sup>

## Necroptosis in Atherosclerosis

The expression of necroptosis mediators RIPK-3 and MLKL is elevated in human atherosclerotic plaques, both at the mRNA and protein level.<sup>37,38</sup> RIPK-3 and MLKL mRNA are specifically upregulated in subjects with unstable compared with stable atherosclerotic plaques.<sup>37</sup> RIPK-3 expression is also elevated in advanced plaques of LDLR<sup>-/-</sup> mice, predominantly in macrophages. Loss of RIPK-3 reduces advanced atherosclerotic lesions in ApoE<sup>-/-</sup> or LDLR<sup>-/-</sup> mice but has no effect on earlier stages of plaque development,<sup>39</sup> suggesting that macrophage necroptosis plays a major role in advanced plaques. Bone marrow transplantation showed that loss of RIPK-3 expression from bone marrow-derived cells is responsible for this atheroprotective effect.<sup>39</sup> Likewise, deletion of MLKL with antisense oligonucleotides or genetic deletion of MLKL reduces the necrotic area in advanced plaques but not in early atherosclerotic plaques of ApoE<sup>-/-</sup> mice.<sup>40,41</sup> These findings clearly illustrate a role for RIPK-3- and MLKL-mediated macrophage necroptosis in atherosclerosis.

Analogous with RIPK-3, RIPK-1 is mainly found in macrophages of human carotid lesions.<sup>42</sup> However, the role of RIPK-1 in atherogenesis is not straightforward and is complicated by 2 intrinsic, albeit conflicting activities, namely a scaffolding function that promotes cell survival versus a kinase activity that triggers cell death. A full RIPK-1 knockout affects both kinase-independent scaffolding functions and kinase-dependent cell death and inflammation.<sup>42</sup> It is worth mentioning that RIPK1<sup>-/-</sup> mice die perinatally due to the loss of prosurvival, RIPK-1-kinase independent signaling, such as the NF- $\kappa$ B pathway.<sup>43</sup> In contrast, mice with a RIPK-1 kinase dead (eg, K45A) or inactivating (eg, S25D) mutation are viable and display no obvious abnormalities. Similarly, mice with a deficiency of RIPK-3 and MLKL, which are key executioners of necroptosis and regulated by RIPK-1 kinase activity, are also viable and healthy. Therefore, inhibition of pathology-associated necroptosis may serve as a therapeutic target. However, in a comparative study using mice with inactive RIPK-1 kinase (RIPK1D138N/D138N), RIPK-3 deficiency (RIPK3<sup>-/-</sup>), and MLKL deficiency (MLKL<sup>-/-</sup>) in several models of necroptosis-related inflammatory diseases, MLKL deficiency offered little protection in a kidney ischemia-reperfusion model and no protection at all in a model of systemic inflammation, as opposed to RIPK1D138N/D138N and RIPK3<sup>-/-</sup> mice.<sup>44</sup> In general, this favors targeting upstream RIPK-1 and RIPK-3 over MLKL. RIPK-3 inhibitors have been developed and have been shown to block necroptosis in vitro and in vivo. However, they induce concentration-dependent apoptosis and, therefore, none

of them moved into clinical trials.<sup>45</sup> In contrast, several specific RIPK-1 kinase inhibitors were safe and well tolerated in phase I (URL: <https://www.clinicaltrials.gov>; Unique identifiers: NCT02302404,<sup>46</sup> NCT03590613 and NCT03305419,<sup>47</sup> and NCT03757325) and phase II clinical trials (URL: <https://www.clinicaltrials.gov>; Unique identifiers: NCT02776033,<sup>48</sup> NCT02903966,<sup>49</sup> and NCT02858492<sup>53</sup>). Because the classical RIPK-1 kinase inhibitor Nec-1s (necrostatin-1s) suffers from selectivity and potency problems in vivo, several research groups have focused on the development of alternative RIPK-1 inhibitors over the past decade. Consequently, a new generation of alternative RIPK-1 kinase inhibitors have recently been developed with increased potency and improved pharmacokinetic profiles as compared to Nec-1s, such as GSK (GlaxoSmithKline) 547, GSK 772, DNL (Denali Therapeutics) 747, DNL758, and GFH (GenFleet Therapeutics) 312, which are currently being tested in animal models and humans.<sup>50-52</sup> After passing phase I safety and tolerability trials, phase II clinical studies were completed to evaluate the effects of GSK 772 on psoriasis, ulcerative colitis, and rheumatoid arthritis (URL: <https://www.clinicaltrials.gov>; Unique identifiers: NCT02776033,<sup>48</sup> NCT02903966,<sup>49</sup> and NCT02858492<sup>53</sup>). Importantly, promising results were reported for GSK 772 in patients with active plaque psoriasis.<sup>48</sup> DNL758/SAR443122 also passed phase I and is currently included in a proof-of-concept study in patients with cutaneous lupus erythematosus (URL: <https://www.clinicaltrials.gov>; Unique identifier: NCT04781816). Furthermore, GFH312 is currently included in a first-in-human trial (URL: <https://www.clinicaltrials.gov>; Unique identifier: NCT04676711). Altogether, RIPK-1 kinase inhibitors are readily moving into clinical stages and are reported to be safe and well tolerated so far, making the kinase activity of RIPK-1 an attractive therapeutic target for necroptosis in atherosclerosis.

Pharmacological inhibition of RIPK-1 by Nec-1s reduces plaque size and promotes plaque stability in ApoE<sup>-/-</sup> mice.<sup>37</sup> Similar observations apply after administration of RIPK-1 antisense oligonucleotides that reduce but do not completely abrogate Ripk-1 expression.<sup>54</sup> Additional in vitro experiments have unraveled the underlying mechanism by which necroptosis is induced in atherosclerosis. During plaque development, oxLDL (oxidized LDL) increases reactive oxygen species (ROS)-mediated RIPK-3 and MLKL gene expression in macrophages, which leads to necroptosis.<sup>37</sup> These findings demonstrate that inhibition of macrophage necroptosis could be a promising therapeutic strategy to prevent the development of a vulnerable plaque. However, ApoE<sup>-/-</sup> RIPK1S25D/S25D mice lacking active RIPK-1 kinase develop larger plaques compared with ApoE<sup>-/-</sup> RIPK1<sup>+/+</sup> controls.<sup>55</sup> Moreover, pharmacological inhibition of RIPK-1 with GSK 547 does not limit atherogenesis in ApoE<sup>-/-</sup> Fbn1<sup>C1039G+/-</sup> mice, a model of advanced

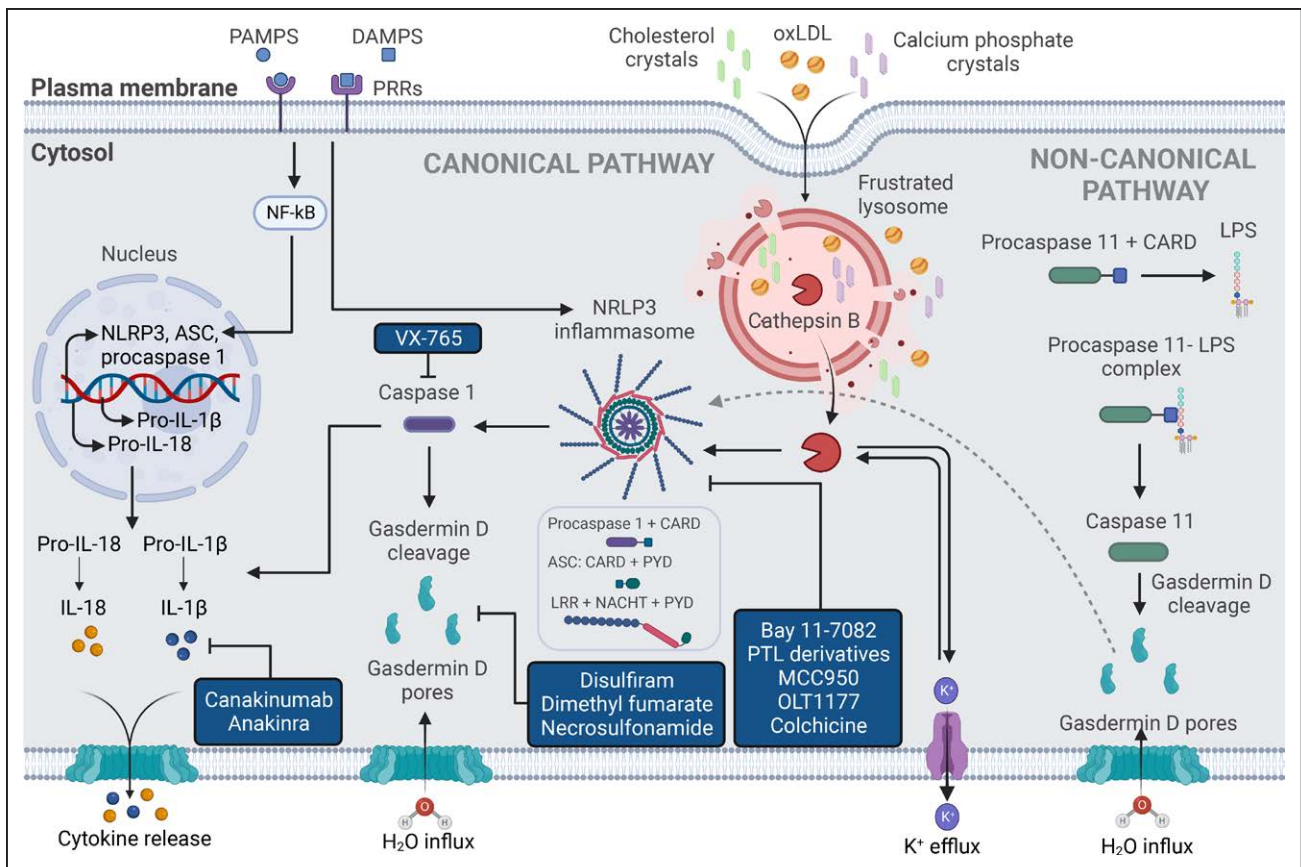


**Figure 3. Overview of NLRP (nucleotide-binding oligomerization domain-like, leucine-rich repeat, and pyrin domain-containing receptor)-3-linked pyroptosis pathways and targets for pharmacological modulation.**

Canonical pyroptosis is characterized by assembly and activation of inflammasomes, which are large supramolecular complexes required for caspase-1 activation. The NLRP-3 inflammasome consists of NLRP3, ASC (apoptosis inhibitor speck-like protein), and procaspase-1. NLRP-3 contains a C-terminal LRR, a central nucleotide domain called NACHT and an N-terminal PYD (pyrin domain). A priming step is required to increase the transcription of pro-IL (interleukin)-1 $\beta$ , NLRP-3, and ASC and is induced by recognition of extracellular molecules, such as lipopolysaccharide (LPS), TNF (tumor necrosis factor)- $\alpha$ , or IL-1 $\beta$  by PRRs (pattern-recognition receptors). Assembly of the inflammasome occurs through ASC which contains a PYD that interacts with the N-terminal PYD in NLRP3, and a CARD (caspase recruitment domain) for binding of procaspase-1. To allow proximity, and hence NLRP-3 activation, between NLRP-3 (mitochondria) and ASC (endoplasmic reticulum), activation of  $\alpha$ -tubulin is required. The latter process can be pharmacologically inhibited by tubulin polymerization inhibitor colchicine. Activation of NLRP3 is induced by low intracellular potassium concentrations, for example, by potassium efflux through ionophores or cation channels. Cathepsins are also required for NLRP-3 activation and are released after lysosomal rupture induced by oxLDL (oxidized low-density lipoprotein), cholesterol, and calcium crystals. Activation of NLRP-3 results in cleavage of procaspase-1 to active caspase-1, which converts pro-IL-1 $\beta$  and pro-IL-18 to their bioactive forms and cleaves GSDMD (gasdermin D) N-terminally (NT). NT-cleaved GSDMDs oligomerize and form NT-GSDMD pores, which allow the secretion of cytokines and eventually results in membrane lysis and cell death. Caspase-1 can be pharmacologically inhibited with VX-765. Pharmacological inhibition of GSDMD can be obtained with disulfiram, dimethyl fumarate or necrosulfonamide. Neutralization of IL-1 $\beta$  with canakinumab or anakinra provides another strategy to block pyroptosis-induced inflammation. Alternatively, pyroptosis can be induced through caspase-11, which can directly sense cytoplasmic LPS without the need for an inflammasome, termed noncanonical pyroptosis. Caspase-11 contains an LPS-binding site located on its CARD domain through which a procaspase-11-LPS complex is formed. Subsequently, caspase-11 is activated which results in NT-cleavage of GSDMD and pyroptotic death. Caspase-11-induced NT-GSDMDs also serves as activator of the NLRP-3 inflammasome thus, caspase-11 indirectly triggers canonical pyroptosis. Image created with Biorender. DAMPs indicates damage-associated molecular patterns; and PAMPs, pathogen-associated molecular patterns.

atherosclerosis.<sup>55</sup> Accordingly, GSK'547 does not limit plaque formation in more advanced stages of atherogenesis while it decreases the plaque area in earlier stages.<sup>56</sup> Additionally, when RIPK-1 expression is reduced by anti-sense oligonucleotides,<sup>54</sup> there is a reduction in the macrophage ability to activate proinflammatory NF- $\kappa$ B while necroptotic cell death remains functional, suggesting RIPK-1 expression may be tightly regulated to balance its proinflammatory versus prodeath functions. Together,

these results stress the complex and stage-dependent involvement of RIPK-1 kinase activity in atherosclerosis.

## PYROPTOSIS

Besides necroptosis, other types of regulated necrosis have been observed in atherosclerotic plaques, although their significance is not always clear-cut. Among the most well-defined is pyroptosis, a proinflammatory form

of regulated cell death that is characterized by the formation of plasma membrane pores via caspase-1-dependent cleavage of GSDMD (gasdermin D), which is highly expressed in different tissues and cell types and well conserved in mammals.<sup>57,58</sup>

### Canonical Inflammasome-Mediated Pyroptosis

Canonical induction of pyroptosis involves cleavage (activation) of caspase-1 through a large supramolecular complex, known as an inflammasome (Figure 3). The NLRP-3 (NOD [nucleotide-binding oligomerization domain]-like, LRR [leucine-rich repeat], and pyrin domain-containing receptor 3) inflammasome is currently the best characterized inflammasome and consists of NLRP-3, ASC (apoptosis-associated speck-like protein containing a caspase recruitment domain), and procaspase-1. First, a priming step, is required to increase the transcription of pro-IL (interleukin)-1 $\beta$ , NLRP-3, and ASC. The priming step is induced by recognition of extracellular molecules, such as lipopolysaccharide, TNF- $\alpha$ , or IL-1 $\beta$  by PRRs (pattern-recognition receptors). Subsequently, NF- $\kappa$ B will be activated and the C-terminal LRR on NLRP3 will be deubiquitinated, allowing NLRP3 activation. Assembly of the inflammasome occurs through ASC which contains a PYD (pyrin domain), that interacts with the N-terminal (NT) PYD in NLRP3, and a CARD (caspase recruitment domain) for binding of procaspase-1.<sup>59</sup>

Once assembled, the NLRP-3 inflammasome can be activated by low intracellular potassium concentrations. Indeed, potassium efflux induced by ionophores such as nigericin or by cation channels such as the P2X7 receptor and TWIK2 channel induced by ATP, are known inducers of NLRP3-dependent pyroptosis.<sup>60,61</sup> Furthermore, cathepsin B is required for NLRP3 activation.<sup>62</sup> Mounting evidence suggests that oxLDL, crystals of cholesterol and calcium phosphate, and fibrillar ligands in atherosclerotic plaques activate NLRP-3 inflammasomes through lysosomal rupture and subsequent cathepsin release, which in turn leads to cleavage and activation of procaspase-1.<sup>63–66</sup> Active caspase-1 exerts proinflammatory effects by converting pro-IL-1 $\beta$  and pro-IL-18 into their bioactive forms. Furthermore, GSDMD is N-terminally cleaved by caspase-1. Subsequently, NT-GSDMDs oligomerize and bind to phospholipids in the cell membrane where they induce pore formation. NT-GSDMD-induced pores are  $\approx$ 10 to 15 nm in diameter, in contrast to the much smaller MLKL-induced channels, and a large number of these NT-GSDMD pores disrupt the plasma membrane and physiological ionic gradients.<sup>67,68</sup> The damaged membrane starts blebbing, a phenomenon that is also observed in apoptotic cells although in a much slower fashion.<sup>67,69</sup> Pyroptotic cells flatten while releasing cellular content through the NT-GSDMD pores, such as IL-1 $\beta$ , IL-18, ATP, HMGB-1, and cleaved GSDMs, which amplify inflammation and pyroptosis induction.<sup>68,69</sup> Interestingly,

secretion of IL-1 $\beta$  and IL-18 does not require cell lysis and is temporally associated with GSDMD-dependent pore formation, suggesting that these pores are sufficient to mediate cytokine release.<sup>70</sup>

### Noncanonical Pyroptosis Induction

Caspase-11 can directly sense cytoplasmic lipopolysaccharide without the need for TLR-4 or a canonical inflammasome, because it contains a lipopolysaccharide-binding site located on its CARD domain, forming a procaspase-11-lipopolysaccharide complex, also called the noncanonical inflammasome (Figure 3).<sup>71</sup> Active caspase-11 cleaves GSDMD which induces pore formation and pyroptosis, similar to caspase-1. Next to direct induction of pyroptosis, caspase-11-induced formation of NT-GSDMD also serves as an activator of the NLRP-3 inflammasome. In this way, caspase-11 indirectly triggers canonical caspase-1-dependent pyroptosis and, subsequently, the maturation and release of IL-1 $\beta$  and IL-18.<sup>72</sup>

### Pyroptosis in Atherosclerosis

Recent studies have shown that components of the NLRP-3 inflammasome are present in human atherosclerotic plaques and are expressed in macrophages and foam cells around the necrotic core.<sup>73,74</sup> Both mRNA and protein levels of NLRP-3, caspase-1, ASC, IL-1 $\beta$ , and IL-18 are increased in human plaques compared with normal arteries.<sup>74–77</sup> In patients with coronary atherosclerosis, the aortic expression of the NLRP-3 inflammasome is correlated with disease severity and clinical risk factors for cardiovascular disease (eg, hypertension, diabetes, smoking, and LDL-cholesterol).<sup>75</sup> Moreover, the highest NLRP3 expression levels were observed in unstable lesions as compared to stable lesions and nonatherosclerotic arteries.<sup>73</sup> All these epidemiological studies highlight a possible role of the NLRP3 inflammasome in atherogenesis and plaque destabilization. Interestingly, it has been demonstrated that ATP and cholesterol crystals induce pyroptosis both in the presence and absence of lipopolysaccharide priming in cultured plaques.<sup>76</sup> Both inducers are relevant in the context of atherosclerosis as cholesterol is involved in every stage of plaque development, while extracellular ATP is expected to be more abundant in advanced stages of plaque development and destabilization due to excessive cell death.<sup>66,76,78</sup> Another possible activator of the NLRP-3 inflammasome in atherosclerosis is nicotine. Indeed, smoking is a major risk factor for atherosclerosis which is at least partly attributable to activation of the ROS/NLRP-3-axis and pyroptosis induction.<sup>79,80</sup>

Many studies have targeted proteins involved in canonical (NLRP3, ASC, caspase-1, IL-1 $\beta$ , and IL-18) and noncanonical (caspase-11) pyroptosis signaling in atherosclerotic models and reported beneficial effects



on atherogenesis (reviewed elsewhere: Xu et al<sup>57</sup> and Qian et al<sup>51</sup>). However, often these targets are not limited to pyroptosis signaling but are also involved in other proinflammatory and cell death pathways. For example, caspase-1 is reported to be proapoptotic, besides its pyroptotic properties, and deletion of caspase-1 activity is linked to lytic, nonpyroptotic cell death.<sup>82</sup> NLRP-3 is also linked to RIPK-1 and RIPK-3 signaling and subsequently, apoptosis and necroptosis.<sup>83–85</sup> In addition, targeting one single player might not suffice as both canonical and noncanonical pathways play a role in atherosclerosis. This is supported by the considerable risk for recurrent cardiovascular events in participants of the CANTOS trial (Canakinumab Anti-inflammatory Thrombosis Outcome Study) treated with the IL-1 $\beta$  antibody canakinumab.<sup>86</sup>

GSDMD is the common executor of both canonical and noncanonical pyroptosis. Interestingly, GSDMD mRNA is upregulated in peripheral blood monocytes of patients with coronary artery disease. Moreover, expression of GSDMD and NT-GSDMD is increased in ApoE<sup>-/-</sup> and wild-type mice fed a high-fat diet as compared to chow-fed controls.<sup>87</sup> Expression of NT-GSDMD was also observed in human endarterectomy specimens.<sup>88</sup> Thus, GSDMD is actively involved in pyroptosis during atherogenesis in both humans and mice, making GSDMD an attractive pharmacological target for pyroptosis in atherosclerosis. Disulfiram is a Food and Drug Administration-approved drug used for the treatment of alcohol abuse and was recently identified as a potent GSDMD inhibitor. It covalently modifies cys191 (in human, cys192 in mouse) in GSDMD to block pore formation at nanomolar concentrations<sup>89</sup> but is metabolized to carbon disulphide, which promotes atherosclerosis, thus not recommended for long-term antiatherosclerosis therapy. Dimethyl fumarate, used as an immunomodulator in multiple sclerosis, has been identified as an alternative GSDMD inhibitor,<sup>90</sup> and reduces aortic plaque area in hyperglycemic ApoE<sup>-/-</sup> mice.<sup>91</sup> More recently, genetic deletion of GSDMD as well as pharmacological inhibition with necrosulfonamide reduce infarct size and heart failure in a mouse model of acute myocardial infarction,<sup>92,93</sup> underlining the involvement of GSDMD in cardiovascular disease and the possibility to use it as a pharmacological target in atherosclerosis. This is supported by the observation that GSDMD deficiency decreases the formation of inflammatory plaques in ApoE<sup>-/-</sup> mice.<sup>88</sup> However, no effect on the initiation and formation of stable aortic plaques was observed. Thus, GSDMD is mainly involved in the transition to an inflammatory, vulnerable plaque phenotype in advanced stages of atherosclerosis and appears to be a promising target for limiting plaque destabilization.

### Gasdermin E-Mediated Secondary Necrosis in Atherosclerosis

Besides the canonical caspase-1/inflammasome pathway that activates GSDMD, GSDME (gasdermin

E) was recently identified as an alternative effector of programmed necrosis under proapoptotic conditions.<sup>94</sup> GSDME leads to membrane pores and programmed necrosis of apoptotic cells, known as secondary necrosis, after cleavage by caspase-3. Efficient clearance of apoptotic cells—a process called efferocytosis—is essential for preventing secondary necrosis. Unfortunately, efferocytosis is strongly impaired in advanced atherosclerosis,<sup>95</sup> making secondary necrosis a main feature of advanced plaques. Stimulation of efferocytosis is challenging as most phagocytes are lipid-filled foam cells with limited phagocytosis potential. Nevertheless, ongoing therapeutic efforts aimed at boosting efferocytosis have shown promising results.<sup>96</sup> It should be noted that GSDME, after cleavage by caspase-3, can also form pores in the mitochondrial membrane resulting in the release of proapoptotic molecules, such as cytochrome c. This event creates a positive feedback loop that promotes caspase-3 activation and further GSDME cleavage, ultimately augmenting apoptotic cell death and secondary necrosis. Surprisingly, there are no studies describing (cleaved) GSDME expression in atherosclerosis. It should be noted that GSDME is transcriptionally controlled by p53 and is essential in the p53-mediated response to DNA damage. Because DNA damage, phosphorylated (active) p53 and cleaved caspase-3 are abundantly present in advanced plaques,<sup>97</sup> this alternative, GSDME-mediated pathway of programmed necrosis, besides GSDMD, definitely needs further attention in the context of atherosclerotic plaque destabilization.

### FERROPTOSIS

Ferroptosis was discovered when the small molecules erastin and RSL (Ras selective lethal)-3 were designed to induce cytotoxicity in cells expressing oncogenic mutant RAS proteins.<sup>98–100</sup> When characterizing the cytotoxicity induced by erastin and (1S,3R)-RSL3, a unique necrotic morphology featuring smaller mitochondria and increased membrane density was observed. Moreover, ferroptosis is characterized by excessive iron-dependent lipid peroxidation. This can occur by enzymatic peroxidation of polyunsaturated fatty acids in phospholipid bilayers through the ACSL (Acyl-CoA synthetase long chain family member)-4/LPCAT (lysophosphatidyl acyltransferase)-3/15-LOX (lipoxygenase) axis (Figure 4). Lipid peroxidation can also be induced nonenzymatically through Fenton chemistry, which forms hydroxyl radicals, and free radical chain reactions. Both enzymatic and nonenzymatic lipid peroxidation require free ferrous iron (Fe<sup>2+</sup>), which resides in a cytosolic labile iron pool. Under physiological conditions, accumulation of ferrous iron in the cytosol and growth of the labile iron pool is limited by ferritin as it can store up to 4500 iron molecules.<sup>101</sup> Another

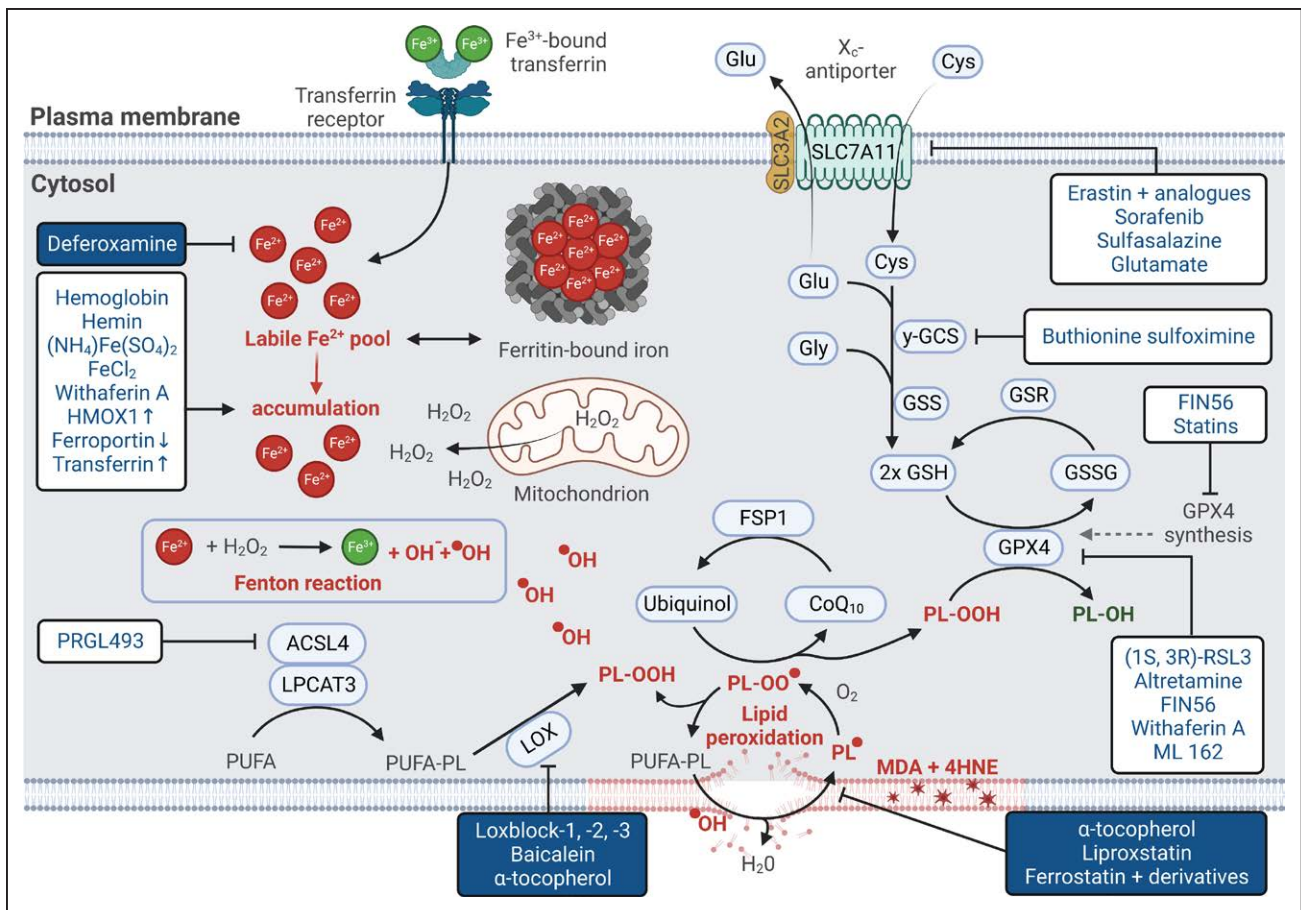


**Figure 4. Overview of ferroptosis-inducing pathways and potential pharmacological targets.**

Ferroptosis is characterized by excessive iron-dependent lipid peroxidation of poly unsaturated fatty acids (PUFAs) in phospholipid (PL) bilayers, which can be induced enzymatically or nonenzymatically and requires free ferrous iron ( $\text{Fe}^{2+}$ ). Enzymatic lipid peroxidation occurs through the ACSL (Acyl-CoA synthetase long chain family member)-4/LPCAT (lysophosphatidyl acyltransferase)-3/15-LOX (lipoyxygenase) axis. Nonenzymatic lipid peroxidation includes Fenton chemistry, which forms hydroxyl radicals, and free radical chain reactions. Free ferrous iron resides in a cytosolic labile iron pool. Growth of the labile iron pool is limited by ferritin, which stores  $\text{Fe}^{2+}$ . When the finely regulated iron balances are disturbed due to overloading of cells with iron, for example, with hemoglobin, hemin, ferrous ammonium sulfate or iron chloride, or due to excessive activation of HMOX (heme oxygenase)-1, decreased ferroportin (iron transporter) expression or enhanced transferrin (iron receptor) expression, the labile iron pool grows beyond the buffering capacities of ferritin, which suffices to induce ferroptosis. Under physiological conditions, lipid peroxides formed in cellular membrane environments are reduced by GPX (glutathione peroxidase)-4, thereby oxidizing glutathione (GSH). For the synthesis of GSH entry of cysteine (Cys) in exchange for glutamate (Glu) through the Xc-antiporter system is required. Inhibition of the Xc-antiporter with erastin, inhibition of glutathione synthesis or direct inhibition of GPX-4 with 1S,3R-RSL3 induces canonical ferroptosis through accumulation of lipid peroxides. Excessive lipid peroxidation of PUFAs in PL bilayers affects chemical and geometric properties of the lipid bilayer which destroys the barrier function of the plasma membrane and leads to cell lysis and eventually cell death. Physiologically ferroptosis is limited by ferritin and by FSP (ferroptosis suppressor protein)-1. FSP-1 reduces coenzyme Q10 ( $\text{CoQ}_{10}$ ) to ubiquinol, which traps lipid peroxy radicals. Pharmacological ferroptosis inhibition is obtained with radical trapping agents, such as  $\alpha$ -tocopherol, lipoxstatin, ferrostatin-1, and derivatives, with iron chelators (eg, deferoxamine) or with blockers of the ACSL-4/LPCAT-3/15-LOX axis (eg, PRGL493, baicalcein,  $\alpha$ -tocopherol, and LOX block-1). GSR indicates glutathion-disulfide reductase; GSS, glutathion synthetase; and GSSG, glutathion disulfide. Image created with Biorender.

ferroptosis limiting factor is FSP (ferroptosis suppressor protein)-1, which reduces coenzyme Q10 to ubiquinol. The latter traps lipid peroxy radicals, accompanied by the formation of coenzyme Q10, thereby preventing the formation of lipid peroxides.<sup>102,103</sup>

When growth of the labile iron pool exceeds the buffering capacity of ferritin (noncanonical pathway) or when formed lipid peroxides are not cleared properly (canonical pathway), excessive lipid peroxidation of polyunsaturated fatty acids in phospholipid bilayers occurs. This affects

the chemical and geometric properties of the lipid bilayer, leads to membrane pore formation, and destroys the barrier function of the plasma membrane. Together, these events lead to cell lysis and eventually cell death.<sup>104</sup> Additionally, lipid peroxides are degraded to toxic lipid aldehydes, such as malondialdehyde and 4-hydroxynonenal, which adds an extra layer of cytotoxicity. Indeed, malondialdehyde and 4-hydroxynonenal easily bind covalently to proteins and DNA, thereby impairing several signaling processes. Furthermore, malondialdehyde binding on

epitopes generates oxidative self-epitopes which can be recognized by scavenger receptors on phagocytes or as DAMPs by PRRs and initiate innate immune responses. Malondialdehyde-modified proteins and lipoproteins also trigger adaptive immune responses.<sup>105</sup> Once lipid peroxides are formed, malondialdehyde and 4-hydroxynonenal may further amplify ROS signaling.

### Canonical Induction of Ferroptosis

Canonical ferroptosis induction involves impaired GPX (glutathione peroxidase)-4, either through direct inhibition of GPX-4 or through depletion of its substrate glutathione (Figure 4).<sup>106</sup> GPX-4 catalyzes the reduction of lipid peroxides in cellular membrane environments and simultaneously oxidizes and consumes glutathione. Full-body depletion of GPX-4 in mice results in embryonic lethality and shRNA mediated GPX-4 knockdown sensitizes cells to undergo ferroptosis, underlining the importance of GPX-4 in normal physiology by preventing excessive lipid peroxidation.<sup>107</sup> (1S,3R)-RSL3 and erastin are both inducers of canonical ferroptosis. (1S,3R)-RSL3 (and not the other diastereomers of RSL3) directly targets and inhibits GPX-4.<sup>107</sup> Erastin inhibits the X<sub>c</sub>-antiporter system which transports cystine, a key precursor in the synthesis of glutathione, into the cell in exchange for glutamate. By inhibiting this system, erastin decreases the entry of cystine into the cell and induces downstream depletion of the cellular antioxidant glutathione, the substrate of GPX-4, thereby impairing GPX-4 activity and triggering accumulation of ROS.<sup>107,108</sup>

### Noncanonical Induction of Ferroptosis

Noncanonical ferroptosis is induced when ferrous iron accumulates in the labile iron pool (Figure 4).<sup>109</sup> This occurs when the finely regulated iron balances are disturbed due to overloading of cells with iron (eg, overload with hemoglobin, hemin, ferrous ammonium sulfate, or iron chloride) or due to excessive activation of HMOX (heme oxygenase)-1, decreased ferroportin expression or enhanced transferrin expression.<sup>109–111</sup> Ferroportin and transferrin regulate iron export to and transport in the circulation, respectively. HMOX-1 is responsible for the catabolism of hemoglobin to heme and Fe<sup>2+</sup>. This is highly relevant in the context of phagocytosis of erythrocytes, a process called erythrophagocytosis, which is responsible for the clearance of aged or damaged erythrocytes by macrophages.<sup>112</sup>

### Ferroptosis in Atherosclerosis

Several epidemiological studies have reported a relationship between iron levels and atherogenesis.<sup>113,114</sup> Indeed, restriction of dietary iron intake or iron chelation with deferoxamine leads to a significant decrease in experimental plaque formation.<sup>115–117</sup> Moreover, iron depletion through

frequent blood donation is associated with a decreased cardiovascular risk.<sup>118–120</sup> Given that lipid peroxidation, intraplaque hemorrhage and iron deposition are key features of advanced human plaques, ferroptosis is suggested to play a role in plaque destabilization, however, to date no direct evidence exists. Erythrocytes are released in the plaque during intraplaque hemorrhages, thereby increasing the cholesterol and iron content of the plaque. Macrophages surrounding intraplaque hemorrhages phagocytose erythrocytes leading to HMOX-1 activation and high intracellular levels of heme and iron.<sup>32,121,122</sup> In vitro experiments demonstrated that erythrophagocytosis by macrophages induces ferroptosis (Puylaert P, unpublished data). The latter results in the release of intracellular content and DAMPs into the plaque, which may contribute to exponential growth of the necrotic core, amplification of the inflammatory cycle, and eventually plaque destabilization. This hypothesis is supported by the observation that atherosclerotic lesions contain malondialdehyde, a toxic lipid peroxidation product, and adaptive IgG antibodies with specificity for malondialdehyde.<sup>105</sup> Malondialdehyde can modify epitopes and is, therefore, capable of inducing undesired proinflammatory responses in atherosclerosis. Malondialdehyde can also bind to LDL, leading to the formation of proatherogenic and immunogenic modified LDL. Interestingly, immunization studies have shown atheroprotective effects of neutralizing endogenous malondialdehyde.<sup>105</sup> Similarly, 4-hydroxynonenal can bind to apolipoprotein B on LDL, which leads to uptake of LDL by macrophages and contributes to foam cell formation. Next to the presence of lipid peroxidation products in plaques, iron-positive foam cells are present in human plaques, HMOX-1 expression is increased in human aortic endothelial cells and hemoglobin, HMOX-1 and ferritin accumulate in advanced human plaques.<sup>32,122,123</sup> These observations are suggestive of growth of the labile iron pool in plaque cells, and thus, combined with lipid peroxidation, of the occurrence of ferroptosis in plaques.

The first specific ferroptosis inhibitors that were identified by high-throughput screening of small molecule libraries are ferrostatin-1 and liproxstatin-1.<sup>106,124</sup> These are potent inhibitors of (1S,3R)-RSL3- and erastin-induced ferroptosis showing EC<sub>50</sub> values in the nanomolar range. The anti-ferroptotic activity of both ferrostatin-1 and liproxstatin-1 can be attributed to their potent radical trapping effects, especially in lipid bilayers.<sup>125,126</sup> Another radical trapping agent that inhibits ferroptosis is  $\alpha$ -tocopherol, albeit with a lower potency in lipid bilayers as compared to ferrostatin-1 and liproxstatin-1. Pharmacological inhibition of ferroptosis with ferrostatin-1 was recently reported to reduce plaque burden in ApoE<sup>-/-</sup> mice as well as in diabetic ApoE<sup>-/-</sup> mice.<sup>123,127</sup> Both studies also observed decreased iron levels in serum and in the aorta and increased GPX-4 and SLC7A11 (subunit of the X<sub>c</sub>-antiporter) expression which, at least partly, explains the observed atheroprotective effects. Accordingly, GPX-4 overexpression in ApoE<sup>-/-</sup> mice inhibited plaque progression.<sup>128</sup> Furthermore,

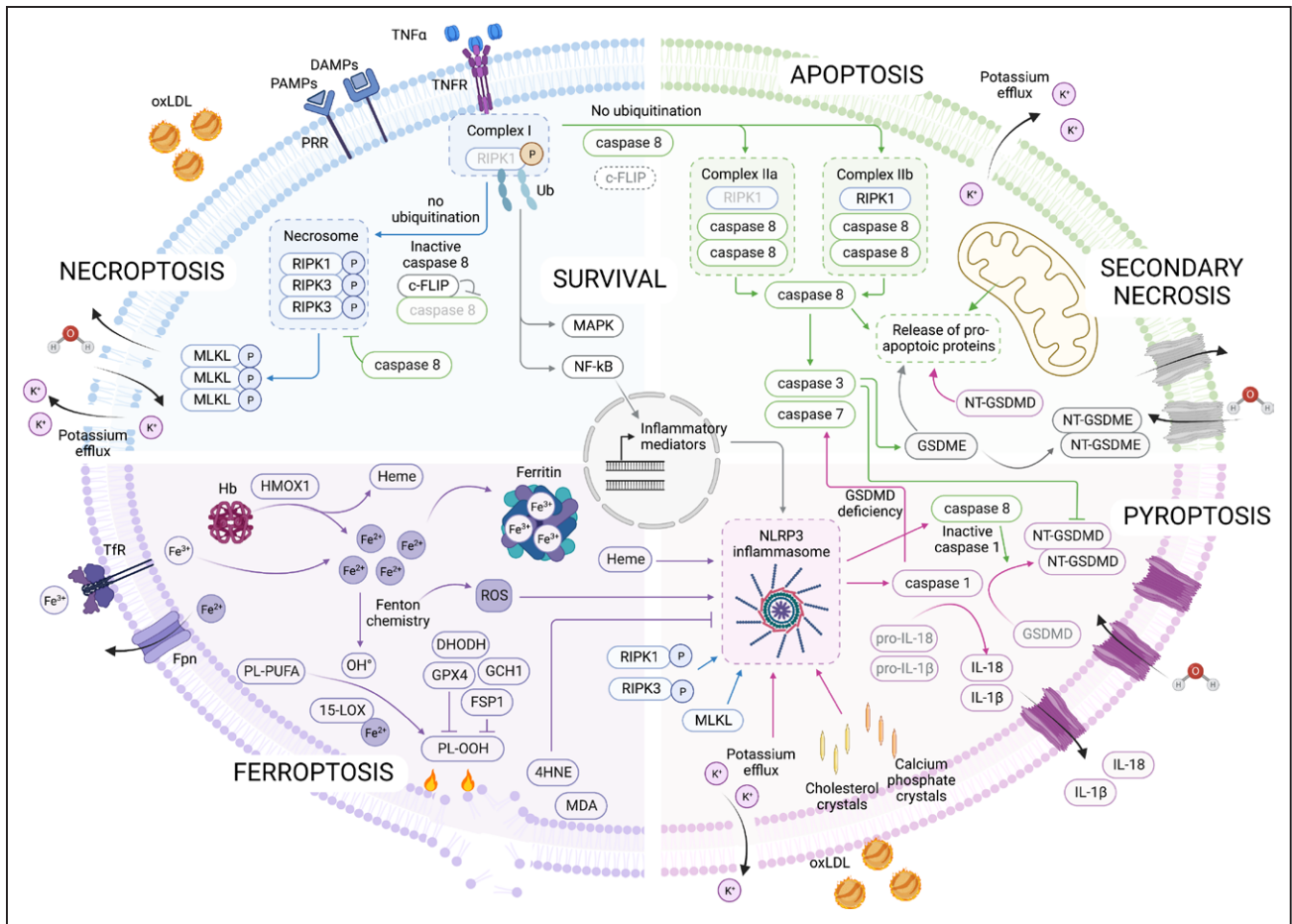


**Figure 5. Cross-talk between necroptosis, apoptosis, secondary necrosis, pyroptosis, and ferroptosis.**

When TNF (tumor necrosis factor)- $\alpha$  binds to its receptor (TNFR) membrane-bound complex I is formed which contains RIPK (receptor-interacting protein kinase)-1. In complex I RIPK-1 is ubiquitinated (Ub) and phosphorylated (P) which keeps it in an inactive conformation. RIPK-1 serves as a scaffold for prosurvival signaling, such as MAPK (mitogen-activated protein kinase) and NF- $\kappa$ B (nuclear factor- $\kappa$ B) pathways. Caspase 8 is inactivated by c-FLIP (cellular FLICE-like protein). When c-FLIP is absent, caspase-8 is released and engages with RIPK-1 to form complex IIa. If RIPK-1 is not ubiquitinated or de-ubiquitinated it is released from complex I and engages with caspase 8 to form complex IIb. Both complex IIa and complex IIb activate caspase 8, which in turn activates apoptosis effector caspases 3 and 7. Caspase-8 also induces the mitochondrial release of proapoptotic proteins. Caspase 3 can cleave GSDME (gasdermin E), thus excessive caspase 3 activation leads to GSDME-mediated secondary necrosis. If RIPK-1 is not ubiquitinated and caspase 8 is inactivated (eg, by c-FLIP), RIPK-1 is released from complex I, undergoes activating autophosphorylations and phosphorylates RIPK-3. Phosphorylated RIPK-1 and RIPK-3 form a necrosome which recruits and phosphorylates MLKL (mixed lineage kinase domain-like protein). Subsequently, oligomerization of MLKL induces membrane permeabilization and eventually necroptosis. During necroptosis, apoptosis and secondary necrosis, potassium efflux occurs which is an activator of the NLRP-3 (NOD [nucleotide-binding oligomerization] domain-like, LRR [leucine-rich repeat]- and pyrin domain-containing receptor 3) inflammasome. Cholesterol crystals indirectly also induce potassium efflux. Caspase 1 is activated on the NLRP-3 inflammasome and in turn cleaves GSDMD (gasdermin D) N-terminally (NT) and activates IL (interleukin)-1 $\beta$  and IL-18. NT-GSDMDs oligomerize and form GSDMD pores leading to osmotic lysis and cytokine release. In the absence of GSDMD, caspase 1 induces apoptosis through activation of caspase 3. Reciprocally, caspase 3 limits pyroptosis through inhibition of GSDMD. In the absence of caspase 1, caspase 8 can also become activated on the NLRP-3 inflammasome and can cleave GSDMD. GSDMD and GSDME can also promote mitochondrial release of proapoptotic proteins, demonstrating intense cross-talk between pyroptosis, apoptosis, and secondary necrosis. Moreover, the necroptosis effector MLKL induces assembly of the NLRP-3 inflammasome, which can be activated by RIPK-1 and RIPK-3. Transcription of NLRP-3 inflammasome components can be induced through NF- $\kappa$ B pathways, linking TNF- $\alpha$  signaling and pyroptosis. Similarly, heme and oxidative stress can also activate the NLRP-3 inflammasome, providing a link between ferroptosis and pyroptosis. Indeed, heme is formed together with ferrous iron (Fe<sup>2+</sup>) when hemoglobin (Hb) is catabolized by HMOX (heme oxygenase)-1. This contributes to growth of the labile iron pool, which is limited by ferritin. Growth of the labile iron pool beyond the buffering capacity of ferritin, for example, by excessive HMOX-1 activation, increased expression of TfR (transferrin receptor) or decreased expression of Fpn (ferroportin), can induce ferroptosis through Fenton chemistry and nonenzymatic lipid peroxidation. Alternatively, enzymatic lipid peroxidation by 15-LOX (lipoxygenase) can also induce ferroptosis. Excessive lipid peroxidation can be limited by GPX (glutathione peroxidase)-4 and FSP (ferroptosis suppressor protein)-1. During lipid peroxidation toxic lipid aldehydes are formed, such as malondialdehyde (MDA) and 4-hydroxynonenal (4-HNE). The latter was recently reported to inhibit NLRP-3 inflammasome activation. These examples illustrate that the fate of a cell depends on many factors (eg, cell death stimulus, cellular environment, cell type, and expression pattern of cell death executors) and is subjected to intense cross-talk between cell death pathways. Image created with Biorender.

**Table 1. Necroptosis-, Pyroptosis-, and Ferroptosis-Related Proteins in Human Atherosclerotic Plaques**

Cell death-related genes and proteins	Expression in human atherosclerotic plaques	Methods	Reference
RIPK-3	Gene expression upregulated in unstable carotid plaques	Gene expression analysis on carotid endarterectomy specimens (n=127 plaques from BiKE) vs disease-free artery (n=10 organ donors without cardiovascular history). Gene expression analysis on unstable (n=87 symptomatic patients) vs stable (n=40 asymptomatic patients) carotid plaques from BiKE.	Karunakaran et al <sup>37</sup> and Perisic et al <sup>134</sup>
	Protein levels increased in carotid lesions with necrotic core	Western blot analysis of plaques with vs without necrotic core (n≥6 per group from 12 autopsy samples and 6 carotid endarterectomies)	Tian et al <sup>38</sup>
RIPK-1	Protein level increased in carotid lesions with necrotic core	Western blot analysis of plaques with vs without necrotic core (n≥6 per group from 12 autopsy samples and 6 carotid endarterectomies)	Tian et al <sup>38</sup>
	Expressed in macrophages (but not smooth muscle cells) in carotid lesions	Double immunofluorescence staining of advanced carotid plaque selected from a library of endarterectomy specimens from patients with carotid stenosis >70%	Coornaert et al <sup>42</sup>
	Expressed in macrophages and endothelial cells in coronary plaques	Immunohistochemical analysis of early plaques vs arteries with pathological intimal thickening obtained from CVPPath Institute Sudden Cardiac Death registry	Karunakaran et al <sup>54</sup> and Arking et al <sup>135</sup>
	Gene expression upregulated in early carotid plaques	Gene expression analysis on carotid endarterectomy specimens from 34 patients: plaque tissue (mostly stage IV and V lesions) vs adjacent macroscopically intact tissue (almost exclusively stage I and II lesions)	Karunakaran et al <sup>54</sup> and Ayari et al <sup>136</sup>
MLKL	Gene expression upregulated in unstable carotid plaques	Gene expression analysis on carotid endarterectomy specimens (n=127 plaques from BiKE) vs disease-free artery (n=10 organ donors without cardiovascular history). Gene expression analysis on unstable (n=87 symptomatic patients) vs stable (n=40 asymptomatic patients) carotid plaques from BiKE.	Karunakaran et al <sup>37</sup> and Perisic et al <sup>134</sup>
	P-MLKL levels increased in advanced coronary plaques	Immunohistochemical analysis of advanced lesions (n=11) vs arteries with pathological intimal thickening (n=5) obtained from CVPPath Institute Sudden Cardiac Death registry	Karunakaran et al <sup>37</sup> and Arking et al <sup>135</sup>
NLRP-3	Gene and protein levels upregulated in unstable carotid plaques	Gene expression analysis on carotid endarterectomy specimens from 30 patients with >70% stenosis: unstable vs stable plaques (n=15 per group) based on plaque morphology. Immunohistochemical analysis of carotid endarterectomy specimens from 30 patients with >70% stenosis vs mesenteric arteries from 10 patients with early intestinal tumors. Western blot and immunohistochemical analysis of carotid endarterectomy specimens from 30 patients with >70% stenosis: unstable vs stable plaques (n=15 per group) based on plaque morphology.	Shi et al <sup>73</sup>
	Gene and protein levels upregulated in advanced coronary plaques	Gene expression analysis and immunohistochemistry of coronary artery specimens from 10 explanted hearts (4 patients undergoing heart transplantation, 6 donor hearts not fulfilling transplantation criteria, all male): advanced (stage IV–VI) vs early (stage I–III) lesions from the same coronary tree (n=10 per group)	Rajamaki et al <sup>74</sup>
	Expressed in aortic plaques and expression level correlated with coronary atherosclerosis severity and risk factors	Immunohistochemical analysis of ascending aorta specimens from 36 patients undergoing coronary artery bypass graft surgery (severity determined using Genini scoring) vs 10 healthy renal arteries from kidney donors	Zheng et al <sup>75</sup>
	Gene levels upregulated in carotid plaques and expressed in intraplaque macrophages and smooth muscle cells	Gene expression analysis on carotid endarterectomy specimens (n=106 plaques from BiKE) vs disease-free arteries (n=9 iliac arteries, n=1 aorta intima from organ donors without cardiovascular history). Immunohistochemical analysis of 3 carotid endarterectomy specimens from BiKE.	Paramel Varghese et al <sup>76</sup>
	Expression positively correlated with degree of stenosis and plaque severity stage	Immunohistochemical analysis of 40 coronary artery samples obtained from 4 autopsy cases (causes of death: occupying lesions, cerebral hemorrhage, myocardial infarction, and diabetes)	Zhou et al <sup>137</sup>
ASC	Gene and protein levels upregulated in unstable carotid plaques	Gene expression analysis on carotid endarterectomy specimens from 30 patients with >70% stenosis: unstable vs stable plaques (n=15 per group) based on plaque morphology. Immunohistochemical analysis of carotid endarterectomy specimens from 30 patients with >70% stenosis vs mesenteric arteries from 10 patients with early intestinal tumors. Western blot and immunohistochemical analysis of carotid endarterectomy specimens from 30 patients with >70% stenosis: unstable vs stable plaques (n=15 per group) based on plaque morphology.	Shi et al <sup>73</sup>
	Gene and protein levels upregulated in advanced coronary plaques	Gene expression analysis and immunohistochemistry of coronary artery specimens from 10 explanted hearts (4 patients undergoing heart transplantation, 6 donor hearts not fulfilling transplantation criteria, all male): advanced (stage IV–VI) vs early (stage I–III) lesions from the same coronary tree (n=10 per group)	Rajamaki et al <sup>74</sup>

(Continued)

Downloaded from <http://ahajournals.org> by on November 9, 2022

**Table 1. Continued**

Cell death-related genes and proteins	Expression in human atherosclerotic plaques	Methods	Reference
	Gene levels upregulated in carotid plaques and expressed in intraplaque macrophages and smooth muscle cells	Gene expression analysis on carotid endarterectomy specimens (n=106 plaques from BiKE) vs disease-free arteries (n=9 iliac arteries, n=1 aorta intima from organ donors without cardiovascular history). Immunohistochemical analysis of 3 carotid endarterectomy specimens from BiKE.	Paramel Varghese et al <sup>76</sup>
Caspase-1	Gene and protein levels upregulated in unstable carotid plaques	Gene expression analysis on carotid endarterectomy specimens from 30 patients with >70% stenosis: unstable vs stable plaques (n=15 per group) based on plaque morphology. Immunohistochemical analysis of carotid endarterectomy specimens from 30 patients with >70% stenosis vs mesenteric arteries from 10 patients with early intestinal tumors. Western blot and immunohistochemical analysis of carotid endarterectomy specimens from 30 patients with >70% stenosis: unstable vs stable plaques (n=15 per group) based on plaque morphology.	Shi et al <sup>73</sup>
	Gene and protein levels upregulated in advanced coronary plaques	Gene expression analysis and immunohistochemistry of coronary artery specimens from 10 explanted hearts (4 patients undergoing heart transplantation, 6 donor hearts not fulfilling transplantation criteria, all male): advanced (stage IV–VI) vs early (stage I–III) lesions from the same coronary tree (n=10 per group)	Rajamaki et al <sup>74</sup>
	Gene levels upregulated in carotid plaques	Gene expression analysis on carotid endarterectomy specimens (n=106 plaques from BiKE) vs disease-free arteries (n=9 iliac arteries, n=1 aorta intima from organ donors without cardiovascular history). Immunohistochemical analysis of 3 carotid endarterectomy specimens from BiKE.	Paramel Varghese et al <sup>76</sup>
	Cleaved caspase-1 upregulated in symptomatic plaques in vascular smooth muscle cells that are transdifferentiating to macrophages	Double immunofluorescence staining of carotid endarterectomy specimens: symptomatic vs asymptomatic patients (n=12 per group) with >70% stenosis	Burger et al <sup>138</sup> and Montecucco et al <sup>139</sup>
	Expression positively correlated with degree of stenosis and plaque severity stage	Immunohistochemical analysis of 40 coronary artery samples obtained from 4 autopsy cases (causes of death: occupying lesions, cerebral hemorrhage, myocardial infarction, and diabetes)	Zhou et al <sup>37</sup>
IL-1β	Gene and protein levels upregulated in unstable carotid plaques	Gene expression analysis on carotid endarterectomy specimens from 30 patients with >70% stenosis: unstable vs stable plaques (n=15 per group) based on plaque morphology. Immunohistochemical analysis of carotid endarterectomy specimens from 30 patients with >70% stenosis vs mesenteric arteries from 10 patients with early intestinal tumors. Western blot and immunohistochemical analysis of carotid endarterectomy specimens from 30 patients with >70% stenosis: unstable vs stable plaques (n=15 per group) based on plaque morphology.	Shi et al <sup>73</sup>
	Gene levels upregulated in carotid plaques	Gene expression analysis on carotid endarterectomy specimens (n=106 plaques from BiKE) vs disease-free arteries (n=9 iliac arteries, n=1 aorta intima from organ donors without cardiovascular history). Immunohistochemical analysis of 3 carotid endarterectomy specimens from BiKE.	Paramel Varghese et al <sup>76</sup>
	Expression increased in symptomatic plaques in vascular smooth muscle cells that are transdifferentiating to macrophages	Double immunofluorescence staining of carotid endarterectomy specimens: symptomatic vs asymptomatic patients (n=12 per group) with >70% stenosis	Burger et al <sup>138</sup> and Montecucco et al <sup>139</sup>
IL-18	Gene and protein levels upregulated in unstable carotid plaques	Gene expression analysis on carotid endarterectomy specimens from 30 patients with >70% stenosis: unstable vs stable plaques (n=15 per group) based on plaque morphology. Immunohistochemical analysis of carotid endarterectomy specimens from 30 patients with >70% stenosis vs mesenteric arteries from 10 patients with early intestinal tumors. Western blot and immunohistochemical analysis of carotid endarterectomy specimens from 30 patients with >70% stenosis: unstable vs stable plaques (n=15 per group) based on plaque morphology.	Shi et al <sup>73</sup>
	Gene levels upregulated in carotid plaques	Gene expression analysis on carotid endarterectomy specimens (n=106 plaques from BiKE) vs disease-free arteries (n=9 iliac arteries, n=1 aorta intima from organ donors without cardiovascular history). Immunohistochemical analysis of 3 carotid endarterectomy specimens from BiKE.	Paramel Varghese et al <sup>76</sup>

(Continued)

**Table 1. Continued**

Cell death-related genes and proteins	Expression in human atherosclerotic plaques	Methods	Reference
	Gene and protein levels upregulated in carotid plaques and correlated with plaque instability	Western blot analysis of 12 endarterectomy specimens (from 40 carotids collected from 35 patients) vs 5 control arteries (2 carotids and 3 mammary arteries collected at autopsy or during coronary artery bypass graft surgery). Immunohistochemical analysis of 6 endarterectomy specimens (from 40 carotids collected from 35 patients). Gene expression analysis on 22 endarterectomy specimens (from 40 carotids collected from 35 patients): symptomatic (n=13) vs asymptomatic (n=9) patients; unstable (n=14) vs stable (n=8) plaques (based on ulceration).	Mallat et al <sup>77</sup>
GSDMD	Cleaved GSDMD expressed in macrophage- and smooth muscle cell-rich areas of advanced carotid plaque	Double immunohistochemical staining of advanced carotid plaque selected from a library of endarterectomy specimens from patients with carotid stenosis >70%	Puylaert et al <sup>88</sup>
PTGS2	Expression positively correlated with degree of stenosis and plaque severity stage	Immunohistochemical analysis of 40 coronary artery samples obtained from 4 autopsy cases (causes of death: occupying lesions, cerebral hemorrhage, myocardial infarction, and diabetes)	Zhou et al <sup>137</sup>
GPX-4	Expression negatively correlated with degree of stenosis and plaque severity stage	Immunohistochemical analysis of 40 coronary artery samples obtained from 4 autopsy cases (causes of death: occupying lesions, cerebral hemorrhage, myocardial infarction, and diabetes)	Zhou et al <sup>137</sup>
Ferritin	Expressed in carotid plaques and upregulated in unstable plaques and symptomatic patients	Immunohistochemical analysis of 52 endarterectomy specimens from patients with >50% stenosis (Linköping Carotid Study): ruptured (n=19) vs vulnerable (n=9) vs stable (n=8) plaques (based on morphology and collagen staining); symptomatic (n=44) vs asymptomatic (n=8) patients	Li et al <sup>140</sup>
	Expressed in early plaques and accumulation in advanced plaques	Immunohistochemical analysis of 35 carotid endarterectomy specimens from patients with varying degree of carotid atherosclerosis (n=18 advanced and ruptured plaques, n=8 early plaques) vs healthy arteries (non-diseased parts of carotid arteries and n=4 mammary artery specimens)	Yuan et al <sup>122</sup>
	Expression in the intima of fatty streaks in areas rich in macrophages and TUNEL positivity	Immunohistochemical analysis of coronary artery and thoracic aorta specimens: fatty streak (n=12 autopsy cases with general atherosclerosis) vs normal arteries (n=19: normal areas of arteries from 12 autopsy cases with general atherosclerosis and 7 young autopsy cases without atherosclerosis)	Yuan <sup>141</sup>
Transferrin receptor	Expressed in carotid plaques and upregulated in unstable plaques and symptomatic patients	Immunohistochemical analysis of 52 endarterectomy specimens from patients with >50% stenosis (Linköping Carotid Study): ruptured (n=19) vs vulnerable (n=9) vs stable (n=8) plaques (based on morphology and collagen staining); symptomatic (n=44) vs asymptomatic (n=8) patients	Li et al <sup>140</sup>
HMOX-1	Gene and protein levels upregulated in symptomatic carotid plaques and correlated with intraplaque iron deposits and hemorrhage	Gene expression analysis on carotid endarterectomy specimens from 4 HeCES patients with bilateral stenosis: symptomatic vs asymptomatic side/plaques Gene expression analysis on carotid endarterectomy specimens from 40 HeCES patients with unilateral stenosis: symptomatic (n=22 patients with ipsilateral stroke symptoms) vs asymptomatic (n=18 patients without cerebrovascular symptoms) Western blot and immunohistochemical analysis of carotid endarterectomy specimens from 22 patients: symptomatic (n=13 patients with confirmed ipsilateral stroke) vs asymptomatic (n=9 asymptomatic patients with normal brain imaging)	Ijäs et al <sup>142</sup>
	Gene expression upregulated in advanced carotid plaques	Gene expression analysis on carotid endarterectomy specimens from 34 patients: plaque tissue (mostly stage IV and V lesions) vs adjacent macroscopically intact tissue (almost exclusively stage I and II lesions)	Ayari et al <sup>136</sup>
	Gene expression upregulated in unstable carotid plaques	Gene expression analysis on unstable (n=40 asymptomatic patients) vs stable (n=87 symptomatic patients) carotid plaques from BiKE	Perisic et al <sup>134</sup>
	Expressed in intraplaque macrophages together with hemoglobin and iron deposits	Immunohistochemical analysis of carotid endarterectomy specimens from 15 patients with >70% stenosis	Kockx et al <sup>32</sup>
	Expressed in atherosclerotic tissue and accumulation in advanced carotid plaques	Combined analysis of: Gene expression in carotid endarterectomy specimens from 34 patients: plaque tissue (mostly stage IV and V lesions) vs adjacent macroscopically intact tissue (almost exclusively stage I and II lesions). Gene expression in carotid endarterectomy specimens from 30 patients with >70% stenosis: advanced (n=8) vs early (n=9) plaques.	Ayari et al, <sup>136</sup> Wu et al, <sup>143</sup> and Döring et al <sup>144</sup>
	Gene expression in coronary plaque areas with hemorrhage	Immunohistochemical analysis of autopsy cases from sudden coronary deaths (CVPath Institute Sudden Coronary Death registry): plaque areas with prior hemorrhage vs areas without hemorrhage	Finn et al <sup>145</sup>

ASC indicates apoptosis-associated speck-like protein; BiKE, Biobank of Karolinska Endarterectomies; GPX, glutathione peroxidase; GSDMD, gasdermin D; HeCES, Helsinki Carotid Endarterectomy Study; HMOX, heme oxygenase; IL, interleukin; MLKL, mixed lineage kinase domain-like protein; NLRP-3, nucleotide-binding oligomerization domain-like, leucine-rich repeat- and pyrin domain-containing receptor 3; PTGS2, prostaglandin-endoperoxide synthase 2; RIPK, receptor-interacting protein kinase; and TUNEL, terminal deoxynucleotidyl transferase dUTP nick-end labeling.

Downloaded from <http://ahajournals.org> by on November 9, 2022

**Table 2. Human Intervention Studies Targeting Necroptosis, Pyroptosis, or Ferroptosis**

Target	Drug	Study	Main findings	Reference
RIPK-1	GSK'772	Phase I single-center, randomized, placebo-controlled, double-blind study in healthy, male, adult volunteers (URL: <a href="https://www.clinicaltrials.gov">https://www.clinicaltrials.gov</a> ; Unique identifier: NCT02302404)	Single and repeated doses were safe and well tolerated. Pharmacokinetic profiles showed dose linearity over the range tested (up to 120 mg bid). High level of RIPK-1 target engagement.	Weisel et al <sup>146</sup>
		Phase IIa multicenter, randomized, placebo-controlled, double-blind, repeat-dose study in patients with mild-to-moderate active plaque-type psoriasis (URL: <a href="https://www.clinicaltrials.gov">https://www.clinicaltrials.gov</a> ; Unique identifier: NCT02776033)	60 mg bid or tid for 84 d was generally safe and well tolerated. Improved clinical efficacy measures and biomarkers in patients with mild-to-moderated active plaque psoriasis.	Weisel et al <sup>148</sup>
		Phase IIa multicenter, randomized, placebo-controlled, double-blind study in patients with active ulcerative colitis (URL: <a href="https://www.clinicaltrials.gov">https://www.clinicaltrials.gov</a> ; Unique identifier: NCT02903966)	60 mg tid for 84 d was generally safe and well tolerated. No clinical improvement in patients with active ulcerative colitis.	Weisel et al <sup>149</sup>
		Phase IIa, multicenter, randomized, placebo-controlled, double-blind study in patients with moderate to severe rheumatoid arthritis (URL: <a href="https://www.clinicaltrials.gov">https://www.clinicaltrials.gov</a> ; Unique identifier: NCT02858492)	60 mg bid or tid for 84 d was generally safe and well tolerated. No clinical improvement in patients with moderate to severe rheumatoid arthritis.	Weisel et al <sup>153</sup>
		Phase I single-center, randomized, placebo-controlled, double-blind study in healthy volunteers in the United Kingdom (URL: <a href="https://www.clinicaltrials.gov">https://www.clinicaltrials.gov</a> ; Unique identifier: NCT03305419) and in Japan (URL: <a href="https://www.clinicaltrials.gov">https://www.clinicaltrials.gov</a> ; Unique identifier: NCT03590613)	Similar pharmacokinetics and tolerability between Western and Japanese subjects	Tompson et al <sup>147</sup>
		Nonrandomized, open-label study to assess the pharmacokinetic profile of a modified-release prototype coated tablet formulation (URL: <a href="https://www.clinicaltrials.gov">https://www.clinicaltrials.gov</a> ; Unique identifier: NCT03649412)	The GSK DiffCORE technology overcame food effects and can be used in once daily dosing regimen	Tompson et al <sup>148</sup>
	GSK3145095	Phase I/II open-label study in patients with solid tumors (URL: <a href="https://www.clinicaltrials.gov">https://www.clinicaltrials.gov</a> ; Unique identifier: NCT03681951)	Study terminated	Cohen et al <sup>147</sup>
	DNL747/SAR443060	Randomized, double-blind, placebo-controlled first-in-human study	Single and multiple ascending dosing 100–400 mg bid for 14 d was generally well tolerated and safe High level of RIPK-1 target engagement. Simultaneous preclinical studies revealed long-term toxicity. Production terminated.	Vissers et al <sup>148</sup>
		Phase Ib multicenter, randomized, double-blind, placebo-controlled crossover study in patients with Alzheimer disease (URL: <a href="https://www.clinicaltrials.gov">https://www.clinicaltrials.gov</a> ; Unique identifier: NCT03757325)	50 mg bid for 28 d was safe and well tolerated High level of RIPK-1 target engagement (but lower than 200 mg bid). Simultaneous preclinical studies revealed long-term toxicity. Production terminated.	Vissers et al <sup>148</sup>
		Phase Ib multicenter, randomized, double-blind, placebo-controlled crossover study in patients with amyotrophic lateral sclerosis (URL: <a href="https://www.clinicaltrials.gov">https://www.clinicaltrials.gov</a> ; Unique identifier: NCT03757351)	50 mg bid for 28 d was safe and well tolerated High level of RIPK-1 target engagement (but lower than 200 mg bid). Simultaneous preclinical studies revealed long-term toxicity. Study terminated.	Vissers et al <sup>148</sup>
	DNL758/SAR443122	Phase IB, randomized, double-blind, placebo-controlled study in hospitalized patients with severe COVID-19 (URL: <a href="https://www.clinicaltrials.gov">https://www.clinicaltrials.gov</a> ; Unique identifier NCT04469621)	300 mg bid for 14 d was considered well tolerated and safe. Preliminary results showed trends towards clinical improvement but a larger confirmatory trial to assess clinically significant effects is required.	Clot et al <sup>149</sup>
		Phase II, multicenter, randomized, double-blind, placebo-controlled proof-of-concept study in patients with moderate to severe subacute or chronic cutaneous lupus erythematosus (URL: <a href="https://www.clinicaltrials.gov">https://www.clinicaltrials.gov</a> ; Unique identifier: NCT04781816)	Ongoing (estimated study completion: March 2023)	
	DNL788/SAR443820	Phase I, open-label, crossover study in healthy volunteers (URL: <a href="https://www.clinicaltrials.gov">https://www.clinicaltrials.gov</a> ; Unique identifier: NCT04982991)	"Robust target engagement was demonstrated at doses that were generally well tolerated." Published on Denali Therapeutics Inc website on October 6, 2021	<sup>150</sup>

(Continued)



**Table 2. Continued**

Target	Drug	Study	Main findings	Reference
		Phase II multicenter, randomized, double-blind, placebo-controlled study in patients with amyotrophic lateral sclerosis (HIMALAYA study, URL: <a href="https://www.clinicaltrials.gov">https://www.clinicaltrials.gov</a> ; Unique identifier: NCT05237284)	Ongoing (estimated study completion: September 2023)	
	GFH312	A first-in-human, randomized, double-blind, placebo-controlled study in healthy subject (URL: <a href="https://www.clinicaltrials.gov">https://www.clinicaltrials.gov</a> ; Unique identifier: NCT04676711)	Ongoing (estimated study completion: August 2022)	
IL-1 $\beta$	Canakinumab	Randomized, double-blind, placebo-controlled, event-driven trial in the prevention of recurrent cardiovascular events among stable post-myocardial infarction patients with hsCRP $\geq$ 2 mg/L (Canakinumab Anti-inflammatory Thrombosis Outcome Study, URL: <a href="https://www.clinicaltrials.gov">https://www.clinicaltrials.gov</a> ; Unique identifier: NCT01327846)	Quarterly subcutaneous administration of 150 mg canakinumab reduced the risk for recurrent cardiovascular events independent of lipid lowering. Quarterly subcutaneous administration of canakinumab decreased hsCRP levels after 48 mo. A residual cardiovascular risk remains in patients despite treatment with high-intensity statins and canakinumab which was associated to IL-18 and IL-6.	Ridker et al <sup>186,151</sup>
NLRP-3 inflammasome	Colchicine (237 clinical trials on <a href="https://www.clinicaltrials.gov">clinicaltrials.gov</a> )	Phase III colchicine cardiovascular outcomes trial (COLCOT, URL: <a href="https://www.clinicaltrials.gov">https://www.clinicaltrials.gov</a> ; Unique identifier: NCT02551094)	Low-dose colchicine (0.5 mg once daily) reduced the risk of ischemic cardiovascular events in patients recruited within 30 d after myocardial infarction. Patients benefit from early initiation of colchicine treatment (time-to-treatment initiation effect).	Tardif et al <sup>152</sup> and Bouabdallaoui et al <sup>153</sup>
		Phase III open-label, randomized, controlled trial to study the effect of low-dose colchicine on the natural history of patients with stable coronary artery disease (LoDoCo, identifier: ACTRN12610000293066)	Addition of 0.5 mg/d colchicine to standard therapy in patients with stable coronary artery disease reduced risk of cardiovascular events	Nidorf et al <sup>154</sup>
		Phase III double-blind, randomized, controlled, investigator-initiated, event-driven trial to study the effect of low-dose colchicine for secondary prevention of cardiovascular disease in patients with established, stable coronary artery disease (LoDoCo2, identifier: ACTRN12614000093684)	Addition of 0.5 mg/d colchicine to standard therapy in patients with stable coronary artery disease decreased the occurrence of cardiovascular events	Nidorf et al <sup>155</sup>
		Phase IV trial of anti-inflammatory therapy during percutaneous coronary intervention (URL: <a href="https://www.clinicaltrials.gov">https://www.clinicaltrials.gov</a> ; Unique identifiers: NCT02594111 and NCT01709981)	No effect on the risk for post-percutaneous coronary intervention-related myocardial infarction. Colchicine attenuated the increase in inflammatory markers after percutaneous coronary intervention.	Shah et al <sup>156</sup>
		Phase IV efficacy and safety study of colchicine in improving the stability of coronary plaques in patients with acute coronary syndrome (COLOCT, URL: <a href="https://www.clinicaltrials.gov">https://www.clinicaltrials.gov</a> ; Unique identifier: NCT04848857)	Ongoing (estimated study completion: July 2023)	
	OLT-1177 (dapansutrile)	Phase I single-center, randomized, dose escalation study in healthy volunteers (URL: <a href="https://www.clinicaltrials.gov">https://www.clinicaltrials.gov</a> ; Unique identifier: NCT02134964)	Daily oral administration of up to 1000 mg for 8 d was generally safe and well tolerated	Marchetti et al <sup>157</sup>
		Phase IIa open-label, dose adaptive, proof-of-concept study in patients with monoarticular gout flare	Orally administered 100–2000 mg/d was generally safe and well tolerated. Reduced target joint pain and joint and systemic inflammation were reported after 7 d treatment.	Klück et al <sup>158</sup>
		Phase Ib single-center, randomized, double-blind study in patients with NYHA II–III systolic heart failure (URL: <a href="https://www.clinicaltrials.gov">https://www.clinicaltrials.gov</a> ; Unique identifier: NCT03534297)	Orally administered 500–2000 mg/d was generally safe and well tolerated in patients with stable HFrEF	Wohlford et al <sup>159</sup>
		Phase 2 pilot, single-center, open-label, proof-of-concept study in patients with Schnitzler syndrome (URL: <a href="https://www.clinicaltrials.gov">https://www.clinicaltrials.gov</a> ; Unique identifier: NCT03595371)	Ongoing (estimated study completion: February 2023)	
		Phase 2 multicenter, randomized, double-blind, placebo-controlled study in patients with moderate COVID-19 symptoms and evidence of early cytokine release syndrome (URL: <a href="https://www.clinicaltrials.gov">https://www.clinicaltrials.gov</a> ; Unique identifier: NCT04540120)	Ongoing (estimated study completion: July 2023)	

(Continued)

**Table 2. Continued**

Target	Drug	Study	Main findings	Reference
Caspase-1	VX765 (belnacasan)	Phase II randomized, double-blind, placebo-controlled study in patients with treatment-resistant partial epilepsy (URL: <a href="https://www.clinicaltrials.gov">https://www.clinicaltrials.gov</a> ; Unique identifier: NCT01048255)	"The primary endpoint of the study was safety and tolerability, and results from the study showed a similar safety profile for VX-765 as compared to placebo. Secondary endpoints and additional analyses evaluated the clinical activity of VX-765, and results support the initiation of a larger and longer-duration." Published on Vertex Pharmaceuticals Inc website on March 10, 2011	<sup>160</sup>
		Phase IIb randomized, double-blind, placebo-controlled, parallel-group, dose-ranging study in patients with treatment-resistant partial epilepsy (URL: <a href="https://www.clinicaltrials.gov">https://www.clinicaltrials.gov</a> ; Unique identifier: NCT01501383)	Terminated	
		Phase II randomized, double-blind, placebo-controlled study in patients with chronic plaque psoriasis requiring systemic therapy (URL: <a href="https://www.clinicaltrials.gov">https://www.clinicaltrials.gov</a> ; Unique identifier: NCT00205465)	Completed: results to be reported	

COLCOT indicates Colchicine Cardiovascular Outcomes Trial; HFrEF, heart failure with reduced ejection fraction; HIMALAYA, Phase 2 Study for SAR443820 in Participants With Amyotrophic Lateral Sclerosis; hsCRP, high-sensitivity C-reactive protein; IL, interleukin; LoDoCo, low dose colchicine; NLRP-3, nucleotide-binding oligomerization domain-like, leucine-rich repeat- and pyrin domain-containing receptor 3; NYHA, New York Heart Association; and RIPK, receptor-interacting protein kinase.

inhibition of enzymatic lipid peroxidation with a pharmacological 15-LOX blocker decreased plaque progression in atherosclerotic rabbits with preestablished plaques and genetic deletion of 15-LOX resulted in decreased plaque burden in ApoE<sup>-/-</sup> mice.<sup>129,130</sup> Together, these studies are highly suggestive of involvement of iron-dependent lipid peroxidation in atherogenesis. Combined with the availability of novel ferrostatin-1 analogs with improved potency and ADME (absorption, distribution, metabolism and excretion) properties, such as UAMC-3203 and UAMC-3206,<sup>131-133</sup> this makes ferroptosis a promising target to explore in atherosclerosis.

## REGULATED NECROSIS IN HUMAN ATHEROSCLEROTIC PLAQUES

As described above, several studies have reported the expression of proteins related to necroptosis, pyroptosis, or ferroptosis in plaques from both humans and animals. Observational studies in human atherosclerotic plaques are summarized in Table 1. Moreover, many compounds targeting regulated necrosis have been developed and some are already moving into clinical trials (Table 2). This

makes targeting necroptosis, pyroptosis, and ferroptosis an interesting approach to explore in atherosclerosis.

## CONCLUDING REMARKS

Research over the past 2 decades has demonstrated that necrotic cell death is critically involved in the formation and destabilization of atherosclerotic plaques. Different forms of regulated necrosis can be distinguished by analyzing a combination of mechanistic characteristics (eg, presence of phosphorylated MLKL during necroptosis and GSDMD-pore formation during pyroptosis) and morphological features (eg, mitochondrial abnormalities during ferroptosis, cytoplasm flattening, and membrane blebbing during pyroptosis). The most prominent characteristics of necroptosis, pyroptosis and ferroptosis are described in Table 3 (and more extensively reviewed elsewhere).<sup>161,162</sup> Hitherto, many qualitative analyses of morphological and mechanistic markers of regulated necrosis in atherosclerotic plaques have been performed. However, a quantitative analysis to estimate the true percentage of intraplaque cells undergoing necroptosis, pyroptosis, and ferroptosis (and hence their contribution to atherogenesis) is currently lacking.

**Table 3. Overview of the Most Prominent Morphological and Mechanistic Characteristics of Necroptosis, Pyroptosis, and Ferroptosis**

	Necroptosis	Pyroptosis	Ferroptosis
Morphological characteristics	Cell swelling	Lack of cell swelling	Mitochondrial abnormalities
	Plasma membrane rupture	Plasma membrane rupture	
	Moderate chromatin condensation	Membrane blebbing and formation of pyroptotic bodies	
		Moderate chromatin condensation	
Mechanistic markers	P-MLKL-mediated membrane disruption	Cleaved GSDMD pores	Lipid peroxidation
			Iron accumulation

GSDMD indicates gasdermin D; and MLKL, mixed lineage kinase domain-like protein.

Pharmacological inhibition of regulated necrosis improves several features of plaque stability, such as lowering plaque inflammation, reducing oxidative stress, and increasing collagen content and fibrous cap thickness. However, different forms of regulated necrosis can occur simultaneously, particularly in advanced atherosclerotic plaques, because of the coordinated action of multiple death-inducing stimuli. Indeed, severity stages in human coronary atherosclerosis positively associate with the expression of both ACSL-4 (ferroptosis), caspase-1, and NLRP-3 (pyroptosis).<sup>137</sup> Furthermore, the expression of several ferroptosis- and necroptosis-related proteins was upregulated in atherosclerotic rabbits and did not respond to atorvastatin or PCSK-9 antibody.<sup>163</sup> This finding highlights the possible contribution of these different forms of regulated necrosis to the residual cardiovascular risk that remains in atherosclerosis patients despite efficient lipid-lowering therapy. Accordingly, it may be necessary to target multiple death pathways. Dimethyl fumarate is a GSDMD inhibitor (pyroptosis) that reduces atherogenesis in hyperglycemic ApoE<sup>-/-</sup> mice by increasing Nrf (nuclear factor erythroid 2-related factor)-2 expression and decreasing ROS production.<sup>91</sup> Nrf2, once activated, binds to the antioxidant responsive element in the nucleus, thereby inducing the expression of antioxidant enzymes, such as HMOX-1.<sup>164</sup> Overexpression of HMOX-1 can trigger noncanonical ferroptosis induction, thus dimethyl fumarate indirectly targets ferroptosis. Moreover, dimethyl fumarate also inhibits NF- $\kappa$ B and promotes apoptosis. Therefore, the atheroprotective effects of dimethyl fumarate treatment are possibly attributable to combined targeting of Nrf-2, ferroptosis, pyroptosis, and apoptosis. Similarly, tanshinone IIA, a flavonoid used in traditional Chinese medicine, has atheroprotective effects due to targeting of either apoptosis,<sup>165</sup> ferroptosis,<sup>166</sup> or NLRP3-mediated pyroptosis.<sup>167</sup>

Another aspect that complicates therapeutic inhibition of regulated necrosis is the cross-talk between cell death mechanisms (Figure 5).<sup>168</sup> Apoptosis, autophagy, and (regulated) necrosis were initially considered mutually exclusive states. However, recent findings reveal a balanced interplay between these types of death so that blocking one type of death may sensitize cells to initiate another death pathway. For example, inhibition of caspases by the pan-caspase-inhibitor zVAD-fmk is sufficient for preventing apoptosis in many experimental models, but it may facilitate the necroptosis program downstream of TNF receptor. Conversely, active caspase-8 promotes apoptosis and simultaneously cleaves RIPK-1 and RIPK-3, thereby preventing activation of the RIPK-1/RIPK-3/MLKL-axis and necroptosis induction.<sup>169,170</sup> These observations underline the fine interplay between apoptosis and necroptosis pathways, with caspase-8 representing the molecular switch.<sup>33</sup> Importantly, caspase-8 can also be activated on inflammasomes when proapoptotic caspase-1 is absent or inhibited.<sup>82</sup> Moreover, necroptosis induction via TLR activation (eg, by poly(I:C) on TLR-3

or by lipopolysaccharide on TLR-4) upregulates the transcription of NLRP-3 while RIPK-1/RIPK-3 signaling can induce NLRP-3 inflammasome activation. During the execution phase of necroptosis, MLKL pores are formed which induce potassium efflux, a known activator of the NLRP-3 inflammasome.<sup>83</sup> Similarly, pannexin-1 channels are formed during apoptosis, which also induce potassium efflux and NLRP-3 inflammasome activation.<sup>171</sup> Altogether, there is a clear overlap and cross-talk between pyroptosis, apoptosis, and necroptosis pathways, which was recently termed PANoptosis.<sup>172</sup> It should be noted, however, that cross-talk with ferroptosis is also described. For example, NLRP3-dependent pyroptosis regulates downstream ferroptosis in a mouse model of type 2 diabetes-induced cardiac remodeling and contractile dysfunction. Moreover, the pyroptosis inhibitors MCC950 and necrosulfonamide inhibit high glucose/high fat-induced ferroptosis in vitro.<sup>173</sup>

In conclusion, the simultaneous occurrence of different types of regulated necrosis and intense cross-talk between cell death pathways provide a strong scientific rationale for recommending combination therapy to prevent necrotic core formation in advanced plaques. Simultaneous inhibition of different types of cell death by combination therapy could be an important emerging concept in the field of atherosclerosis, but so far there is little experimental evidence to support this approach.

## ARTICLE INFORMATION

Received July 13, 2022; accepted September 7, 2022.

### Affiliations

Laboratory of Physiopharmacology and Infla-Med Centre of Excellence, University of Antwerp, Belgium (P.P., M.Z., G.R.Y.D.M., W.M.). Department of Biochemistry, Microbiology and Immunology and Centre for Infection, Immunity and Inflammation, Faculty of Medicine, University of Ottawa, ON, Canada (K.J.R.). University of Ottawa Heart Institute, ON, Canada (K.J.R.).

### Sources of Funding

This work was supported by the Fund for Scientific Research (FWO)-Flanders (EOS 30826052). P. Puylaert is a fellow of the FWO-Flanders.

### Disclosures

None.

## REFERENCES

1. Libby P. Mechanisms of acute coronary syndromes and their implications for therapy. *N Engl J Med*. 2013;368:2004–2013. doi: 10.1056/NEJMr1216063
2. Vincent J. Lipid lowering therapy for atherosclerotic cardiovascular disease: it is not so simple. *Clin Pharmacol Ther*. 2018;104:220–224. doi: 10.1002/cpt.1138
3. Kockx MM, Herman AG. Apoptosis in atherosclerosis: beneficial or detrimental?. *Cardiovasc Res*. 2000;45:736–746. doi: 10.1016/s0008-6363(99)00235-7
4. Crisby M, Kallin B, Thyberg J, Zhivotovsky B, Orrenius S, Kostulas V, Nilsson J. Cell death in human atherosclerotic plaques involves both oncosis and apoptosis. *Atherosclerosis*. 1997;130:17–27. doi: 10.1016/s0021-9150(96)06037-6
5. Kockx MM, De Meyer GR, Muhring J, Jacob W, Bult H, Herman AG. Apoptosis and related proteins in different stages of human

- atherosclerotic plaques. *Circulation*. 1998;97:2307–2315. doi: 10.1161/01.cir.97.23.2307
6. Majno G, Joris I. Apoptosis, oncosis, and necrosis. an overview of cell death. *Am J Pathol*. 1995;146:3–15.
  7. Tabas I. Consequences and therapeutic implications of macrophage apoptosis in atherosclerosis: the importance of lesion stage and phagocytic efficiency. *Arterioscler Thromb Vasc Biol*. 2005;25:2255–2264. doi: 10.1161/01.ATV.0000184783.04864.9f.
  8. Virmani R, Burke AP, Farb A, Kolodgie FD. Pathology of the vulnerable plaque. *J Am Coll Cardiol*. 2006;47:C13–C18. doi: 10.1016/j.jacc.2005.10.065
  9. Virmani R, Kolodgie FD, Burke AP, Farb A, Schwartz SM. Lessons from sudden coronary death: a comprehensive morphological classification scheme for atherosclerotic lesions. *Arterioscler Thromb Vasc Biol*. 2000;20:1262–1275. doi: 10.1161/01.atv.20.5.1262
  10. Kolodgie FD, Gold HK, Burke AP, Fowler DR, Kruth HS, Weber DK, Farb A, Guerrero LJ, Hayase M, Kutys R, et al. Intraplaque hemorrhage and progression of coronary atheroma. *N Engl J Med*. 2003;349:2316–2325. doi: 10.1056/NEJMoa035655
  11. Fernández-Ortiz A, Badimon JJ, Falk E, Fuster V, Meyer B, Mailhac A, Weng D, Shah PK, Badimon L. Characterization of the relative thrombogenicity of atherosclerotic plaque components: implications for consequences of plaque rupture. *J Am Coll Cardiol*. 1994;23:1562–1569. doi: 10.1016/0735-1097(94)90657-2
  12. Seimon T, Tabas I. Mechanisms and consequences of macrophage apoptosis in atherosclerosis. *J Lipid Res*. 2009;50:S382–S387. doi: 10.1194/jlr.R800032-JLR200
  13. Kalinina N, Agrotis A, Antropova Y, DiVitto G, Kanellakis P, Kostolias G, Ilyinskaya O, Tararak E, Bobik A. Increased expression of the DNA-binding cytokine HMGB1 in human atherosclerotic lesions: role of activated macrophages and cytokines. *Arterioscler Thromb Vasc Biol*. 2004;24:2320–2325. doi: 10.1161/01.ATV.0000145573.36113.8a
  14. de Souza AW, Westra J, Limburg PC, Bijl M, Kallenberg CG. HMGB1 in vascular diseases: its role in vascular inflammation and atherosclerosis. *Autoimmun Rev*. 2012;11:909–917. doi: 10.1016/j.autrev.2012.03.007
  15. Kanellakis P, Agrotis A, Kyaw TS, Koulis C, Ahrens I, Mori S, Takahashi HK, Liu K, Peter K, Nishibori M, et al. High-mobility group box protein 1 neutralization reduces development of diet-induced atherosclerosis in apolipoprotein e-deficient mice. *Arterioscler Thromb Vasc Biol*. 2011;31:313–319. doi: 10.1161/atvbaha.110.218669
  16. Cuccurullo C, Iezzi A, Fazio ML, De Cesare D, Di Francesco A, Muraro R, Bei R, Uchino S, Spigonardo F, Chiarelli F, et al. Suppression of RAGE as a basis of simvastatin-dependent plaque stabilization in type 2 diabetes. *Arterioscler Thromb Vasc Biol*. 2006;26:2716–2723. doi: 10.1161/01.atv.0000249630.02085.12
  17. Calkin AC, Giunti S, Sheehy KJ, Chew C, Boolell V, Rajaram YS, Cooper ME, Jandeleit-Dahm KA. The HMG-CoA reductase inhibitor rosuvastatin and the angiotensin receptor antagonist candesartan attenuate atherosclerosis in an apolipoprotein E-deficient mouse model of diabetes via effects on advanced glycation, oxidative stress and inflammation. *Diabetologia*. 2008;51:1731–1740. doi: 10.1007/s00125-008-1060-6
  18. Yin YX, Yao YM, Liu RM, Zhai HX, Li L, Zhang JJ, Chen HW, Wang L, Li N, Xia YF. [The effect of simvastatin on the expression of high mobility group box-1 protein in atherosclerotic rats]. *Zhongguo wei zhong bing ji jiu yi xue = Chinese critical care medicine = Zhongguo weizhongbing jijiuyixue*. 2010;22:306–308.
  19. Bennett MR, Clarke MC. Basic research: killing the old: cell senescence in atherosclerosis. *Nat Rev Cardiol*. 2016;14:8–9. doi: 10.1038/nrcardio.2016.195
  20. Stojanović SD, Fiedler J, Bauersachs J, Thum T, Sedding DG. Senescence-induced inflammation: an important player and key therapeutic target in atherosclerosis. *Eur Heart J*. 2020;41:2983–2996. doi: 10.1093/eurheartj/ehz919
  21. Bennett MR, Sinha S, Owens GK. Vascular smooth muscle cells in atherosclerosis. *Circ Res*. 2016;118:692–702. doi: 10.1161/circresaha.115.306361
  22. Degterev A, Huang Z, Boyce M, Li Y, Jagtap P, Mizushima N, Cuny GD, Mitchison TJ, Moskowitz MA, Yuan J. Chemical inhibitor of nonapoptotic cell death with therapeutic potential for ischemic brain injury. *Nat Chem Biol*. 2005;1:112–119. doi: 10.1038/nchembio711
  23. Degterev A, Hitomi J, Germscheid M, Ch'en IL, Korkina O, Teng X, Abbott D, Cuny GD, Yuan C, Wagner G, et al. Identification of RIP1 kinase as a specific cellular target of necrostatins. *Nat Chem Biol*. 2008;4:313–321. doi: 10.1038/nchembio.83
  24. Cho YS, Challa S, Moquin D, Genga R, Ray TD, Guildford M, Chan FK. Phosphorylation-driven assembly of the RIP1-RIP3 complex regulates programmed necrosis and virus-induced inflammation. *Cell*. 2009;137:1112–1123. doi: 10.1016/j.cell.2009.05.037
  25. He S, Wang L, Miao L, Wang T, Du F, Zhao L, Wang X. Receptor interacting protein kinase-3 determines cellular necrotic response to TNF- $\alpha$ . *Cell*. 2009;137:1100–1111. doi: 10.1016/j.cell.2009.05.021
  26. Zhang DW, Shao J, Lin J, Zhang N, Lu BJ, Lin SC, Dong MQ, Han J. RIP3, an energy metabolism regulator that switches TNF-induced cell death from apoptosis to necrosis. *Science*. 2009;325:332–336. doi: 10.1126/science.1172308
  27. Dondelinger Y, Declercq W, Montessuit S, Roelandt R, Goncalves A, Bruggeman I, Hulpiu P, Weber K, Sehon CA, Marquis RW, et al. MLKL compromises plasma membrane integrity by binding to phosphatidylinositol phosphates. *Cell Rep*. 2014;7:971–981. doi: 10.1016/j.celrep.2014.04.026
  28. Vanden Berghe T, Linkermann A, Jouan-Lanhouet S, Walczak H, Vandenabeele P. Regulated necrosis: the expanding network of non-apoptotic cell death pathways. *Nat Rev Mol Cell Biol*. 2014;15:135–147. doi: 10.1038/nrm3737
  29. Delanghe T, Dondelinger Y, Bertrand MJM. RIPK1 kinase-dependent death: a symphony of phosphorylation events. *Trends Cell Biol*. 2020;30:189–200. doi: 10.1016/j.tcb.2019.12.009
  30. Declercq W, Vanden Berghe T, Vandenabeele P. RIP kinases at the crossroads of cell death and survival. *Cell*. 2009;138:229–232. doi: 10.1016/j.cell.2009.07.006
  31. Wang L, Du F, Wang X. TNF- $\alpha$  induces two distinct caspase-8 activation pathways. *Cell*. 2008;133:693–703. doi: 10.1016/j.cell.2008.03.036
  32. Kockx MM, Cromheeke KM, Knaepen MW, Bosmans JM, De Meyer GR, Herman AG, Bult H. Phagocytosis and macrophage activation associated with hemorrhagic microvessels in human atherosclerosis. *Arterioscler Thromb Vasc Biol*. 2003;23:440–446. doi: 10.1161/01.ATV.0000057807.28754.7f
  33. Fritsch M, Günther SD, Schwarzer R, Albert MC, Schorn F, Werthenbach JP, Schiffmann LM, Stair N, Stocks H, Seeger JM, et al. Caspase-8 is the molecular switch for apoptosis, necroptosis and pyroptosis. *Nature*. 2019;575:683–687. doi: 10.1038/s41586-019-1770-6
  34. Petrie EJ, Czabotar PE, Murphy JM. The structural basis of necroptotic cell death signaling. *Trends Biochem Sci*. 2019;44:53–63. doi: 10.1016/j.tics.2018.11.002
  35. Sun X, Yin J, Starovasnik MA, Fairbrother WJ, Dixit VM. Identification of a novel homotypic interaction motif required for the phosphorylation of receptor-interacting protein (RIP) by RIP3. *J Biol Chem*. 2002;277:9505–9511. doi: 10.1074/jbc.M109488200
  36. Wang H, Sun L, Su L, Rizo J, Liu L, Wang LF, Wang FS, Wang X. Mixed lineage kinase domain-like protein MLKL causes necrotic membrane disruption upon phosphorylation by RIP3. *Mol Cell*. 2014;54:133–146. doi: 10.1016/j.molcel.2014.03.003
  37. Karunakaran D, Geoffrion M, Wei L, Gan W, Richards L, Shangari P, DeKemp EM, Beanlands RA, Perisic L, Maegdefessel L, et al. Targeting macrophage necroptosis for therapeutic and diagnostic interventions in atherosclerosis. *Sci Adv*. 2016;2:e1600224. doi: 10.1126/sciadv.1600224
  38. Tian F, Yao J, Yan M, Sun X, Wang W, Gao W, Tian Z, Guo S, Dong Z, Li B, et al. 5-aminolevulinic acid-mediated sonodynamic therapy inhibits RIPK1/RIPK3-dependent necroptosis in THP-1-derived foam cells. *Sci Rep*. 2016;6:21992. doi: 10.1038/srep21992
  39. Lin J, Li H, Yang M, Ren J, Huang Z, Han F, Huang J, Ma J, Zhang D, Zhang Z, et al. A role of RIP3-mediated macrophage necrosis in atherosclerosis development. *Cell Rep*. 2013;3:200–210. doi: 10.1016/j.celrep.2012.12.012
  40. Rasheed A, Robichaud S, Nguyen MA, Geoffrion M, Wyatt H, Cottee ML, Dennison T, Pietrangelo A, Lee R, Lagace TA, et al. Loss of MLKL (Mixed Lineage Kinase Domain-Like Protein) decreases necrotic core but increases macrophage lipid accumulation in atherosclerosis. *Arterioscler Thromb Vasc Biol*. 2020;40:1155–1167. doi: 10.1161/atvbaha.119.313640
  41. Hosseini Z, Marinello M, Decker C, Sansbury BE, Sadhu S, Gerlach BD, Bossardi Ramos R, Adam AP, Spite M, Fredman G. Resolvin D1 enhances necroptotic cell clearance through promoting macrophage fatty acid oxidation and oxidative phosphorylation. *Arterioscler Thromb Vasc Biol*. 2021;41:1062–1075. doi: 10.1161/atvbaha.120.315758
  42. Coornaert I, Puylaert P, Marcasoli G, Grootaert MOJ, Vandenabeele P, De Meyer GRY, Martinet W. Impact of myeloid RIPK1 gene deletion on atherogenesis in ApoE-deficient mice. *Atherosclerosis*. 2021;322:51–60. doi: 10.1016/j.atherosclerosis.2021.02.021
  43. Kelliher MA, Grimm S, Ishida Y, Kuo F, Stanger BZ, Leder P. The death domain kinase RIP mediates the TNF-induced NF- $\kappa$ B signal. *Immunity*. 1998;8:297–303. doi: 10.1016/s1074-7613(00)80535-x
  44. Newton K, Dugger DL, Maltzman A, Greve JM, Hedehus M, Martin-McNulty B, Carano RA, Cao TC, van Bruggen N, Bernstein L, et al. RIPK3 deficiency or catalytically inactive RIPK1 provides greater benefit

- than MLKL deficiency in mouse models of inflammation and tissue injury. *Cell Death Differ*. 2016;23:1565–1576. doi: 10.1038/cdd.2016.46
45. Mandal P, Berger SB, Pillay S, Moriwaki K, Huang C, Guo H, Lich JD, Finger J, Kasparcova V, Votta B. et al. RIP3 induces apoptosis independent of proinflammatory kinase activity. *Mol Cell*. 2014;56:481–495. doi: 10.1016/j.molcel.2014.10.021
  46. Weisel K, Scott NE, Tompson DJ, Votta BJ, Madhavan S, Povey K, Wolstenholme A, Simeoni M, Rudo T, Richards-Peterson L. et al. Randomized clinical study of safety, pharmacokinetics, and pharmacodynamics of RIPK1 inhibitor GSK2982772 in healthy volunteers. *Pharmacol Res Perspect*. 2017;5:e00365. doi: 10.1002/prp2.365
  47. Tompson DJ, Davies C, Scott NE, Cannons EP, Kostapanos M, Gross AS, Powell M, Ino H, Shimamura R, Ogura H. et al. Comparison of the pharmacokinetics of RIPK1 inhibitor GSK2982772 in healthy western and Japanese subjects. *Eur J Drug Metab Pharmacokinet*. 2021;46:71–83. doi: 10.1007/s13318-020-00652-2
  48. Weisel K, Berger S, Papp K, Maari C, Krueger JG, Scott N, Tompson D, Wang S, Simeoni M, Bertin J. et al. Response to inhibition of receptor-interacting protein kinase 1 (RIPK1) in active plaque psoriasis: a randomized placebo-controlled study. *Clin Pharmacol Ther*. 2020;108:808–816. doi: 10.1002/cpt.1852
  49. Weisel K, Scott N, Berger S, Wang S, Brown K, Powell M, Broer M, Watts C, Tompson DJ, Burriss SW. et al. A randomised, placebo-controlled study of RIPK1 inhibitor GSK2982772 in patients with active ulcerative colitis. *BMJ Open Gastroenterol*. 2021;8:e000680. doi: 10.1136/bmjgast-2021-000680
  50. Harris PA, Berger SB, Jeong JU, Nagilla R, Bandyopadhyay D, Campobasso N, Capriotti CA, Cox JA, Dare L, Dong X. et al. Discovery of a first-in-class receptor interacting protein 1 (rip1) kinase specific clinical candidate (gsk2982772) for the treatment of inflammatory diseases. *J Med Chem*. 2017;60:1247–1261. doi: 10.1021/acs.jmedchem.6b01751
  51. Wang W, Marinis JM, Beal AM, Savadkar S, Wu Y, Khan M, Taunk PS, Wu N, Su W, Wu J. et al. RIP1 kinase drives macrophage-mediated adaptive immune tolerance in pancreatic cancer. *Cancer Cell*. 2018;34:757–774. e757. doi: 10.1016/j.ccell.2018.10.006
  52. Mifflin L, Ofengeim D, Yuan J. Receptor-interacting protein kinase 1 (RIPK1) as a therapeutic target. *Nat Rev Drug Discov*. 2020;19:553–571. doi: 10.1038/s41573-020-0071-y
  53. Weisel K, Berger S, Thorn K, Taylor PC, Peterfy C, Siddall H, Tompson D, Wang S, Quattrocchi E, Burriss SW. et al. A randomized, placebo-controlled experimental medicine study of RIPK1 inhibitor GSK2982772 in patients with moderate to severe rheumatoid arthritis. *Arthritis Res Ther*. 2021;23:85. doi: 10.1186/s13075-021-02468-0
  54. Karunakaran D, Nguyen MA, Geoffrin M, Vreeken D, Lister Z, Cheng HS, Otte N, Essebier P, Wyatt H, Kandiah JW. et al. RIPK1 expression associates with inflammation in early atherosclerosis in humans and can be therapeutically silenced to reduce NF- $\kappa$ B activation and atherogenesis in mice. *Circulation*. 2021;143:163–177. doi: 10.1161/circulationaha.118.038379
  55. Puylaert P, Coornaert I, Neutel CHG, Dondelinger Y, Delanghe T, Bertrand MJM, Guns P-J, De Meyer GRY, Martinet W. The impact of RIPK1 kinase inhibition on atherogenesis: a genetic and a pharmacological approach. *Biomedicines*. 2022;10:1016. doi: 10.3390/biomedicines10051016
  56. Zhang Y, Li H, Huang Y, Chen H, Rao H, Yang G, Wan Q, Peng Z, Bertin J, Geddes B. et al. Stage-dependent impact of RIPK1 inhibition on atherogenesis: dual effects on inflammation and foam cell dynamics. *Front Cardiovasc Med*. 2021;8:715337. doi: 10.3389/fcvm.2021.715337
  57. Xu YJ, Zheng L, Hu YW, Wang Q. Pyroptosis and its relationship to atherosclerosis. *Clin Chim Acta*. 2018;476:28–37. doi: 10.1016/j.cca.2017.11.005
  58. Shi J, Gao W, Shao F. Pyroptosis: gasdermin-mediated programmed necrotic cell death. *Trends Biochem Sci*. 2017;42:245–254. doi: 10.1016/j.tibs.2016.10.004
  59. Martinet W, Coornaert I, Puylaert P, De Meyer GRY. Macrophage death as a pharmacological target in atherosclerosis. *Front Pharmacol*. 2019;10:306. doi: 10.3389/fphar.2019.00306
  60. Di A, Xiong S, Ye Z, Malireddi RKS, Kometani S, Zhong M, Mittal M, Hong Z, Kanneganti TD, Rehman J. et al. The TWIK2 potassium efflux channel in macrophages mediates NLRP3 inflammasome-induced inflammation. *Immunity*. 2018;49:56–65.e54. doi: 10.1016/j.immuni.2018.04.032
  61. Pétrilli V, Papin S, Dostert C, Mayor A, Martinon F, Tschopp J. Activation of the NALP3 inflammasome is triggered by low intracellular potassium concentration. *Cell Death Differ*. 2007;14:1583–1589. doi: 10.1038/sj.cdd.4402195
  62. Chevriaux A, Pilot T, Derangère V, Simonin H, Martine P, Chalmin F, Ghiringhelli F, Rébé C. Cathepsin B is required for NLRP3 inflammasome activation in macrophages, through NLRP3 interaction. *Front Cell Dev Biol*. 2020;8:167. doi: 10.3389/fcell.2020.00167
  63. Lin J, Shou X, Mao X, Dong J, Mohabeer N, Kushwaha KK, Wang L, Su Y, Fang H, Li D. Oxidized low density lipoprotein induced caspase-1 mediated pyroptotic cell death in macrophages: implication in lesion instability?. *PLoS One*. 2013;8:e62148. doi: 10.1371/journal.pone.0062148
  64. Karasawa T, Takahashi M. The crystal-induced activation of NLRP3 inflammasomes in atherosclerosis. *Inflamm Regen*. 2017;37:18. doi: 10.1186/s41232-017-0050-9
  65. Grebe A, Hoss F, Latz E. NLRP3 Inflammasome and the IL-1 pathway in atherosclerosis. *Circ Res*. 2018;122:1722–1740. doi: 10.1161/CIRCRESAHA.118.311362
  66. Duewell P, Kono H, Rayner KJ, Sirois CM, Vladimer G, Bauernfeind FG, Abela GS, Franchi L, Nunez G, Schnurr M. et al. NLRP3 inflammasomes are required for atherogenesis and activated by cholesterol crystals. *Nature*. 2010;464:1357–1361. doi: 10.1038/nature08938
  67. Chen X, He WT, Hu L, Li J, Fang Y, Wang X, Xu X, Wang Z, Huang K, Han J. Pyroptosis is driven by non-selective gasdermin-D pore and its morphology is different from MLKL channel-mediated necroptosis. *Cell Res*. 2016;26:1007–1020. doi: 10.1038/cr.2016.100
  68. Xia S, Zhang Z, Magupalli VG, Pablo JL, Dong Y, Vora SM, Wang L, Fu TM, Jacobson MP, Greka A. et al. Gasdermin D pore structure reveals preferential release of mature interleukin-1. *Nature*. 2021;593:607–611. doi: 10.1038/s41586-021-03478-3
  69. Liu X, Xia S, Zhang Z, Wu H, Lieberman J. Channelling inflammation: gasdermins in physiology and disease. *Nat Rev Drug Discov*. 2021;20:384–405. doi: 10.1038/s41573-021-00154-z
  70. Evavold CL, Ruan J, Tan Y, Xia S, Wu H, Kagan JC. The pore-forming protein gasdermin d regulates interleukin-1 secretion from living macrophages. *Immunity*. 2018;48:35–44.e36. doi: 10.1016/j.immuni.2017.11.013
  71. Huang X, Feng Y, Xiong G, Whyte S, Duan J, Yang Y, Wang K, Yang S, Geng Y, Ou Y. et al. Caspase-11, a specific sensor for intracellular lipopolysaccharide recognition, mediates the non-canonical inflammatory pathway of pyroptosis. *Cell Biosci*. 2019;9:31. doi: 10.1186/s13578-019-0292-0
  72. Kayagaki N, Stowe IB, Lee BL, O'Rourke K, Anderson K, Warming S, Cuellar T, Haley B, Roose-Girma M, Phung QT. et al. Caspase-11 cleaves gasdermin D for non-canonical inflammasome signalling. *Nature*. 2015;526:666–671. doi: 10.1038/nature15541
  73. Shi X, Xie WL, Kong WW, Chen D, Qu P. Expression of the NLRP3 inflammasome in carotid atherosclerosis. *J Stroke Cerebrovasc Dis*. 2015;24:2455–2466. doi: 10.1016/j.jstrokecerebrovasdis.2015.03.024
  74. Rajamaki K, Mayranpaa MI, Risco A, Tuimala J, Nurmi K, Cuenda A, Eklund KK, Oorni K, Kovanen PT. p38delta MAPK: a novel regulator of NLRP3 inflammasome activation with increased expression in coronary atherogenesis. *Arterioscler Thromb Vasc Biol*. 2016;36:1937–1946. doi: 10.1161/atvbaha.115.307312
  75. Zheng F, Xing S, Gong Z, Xing Q. NLRP3 inflammasomes show high expression in aorta of patients with atherosclerosis. *Heart Lung Circ*. 2013;22:746–750. doi: 10.1016/j.hlc.2013.01.012
  76. Paramel Varghese G, Folkersen L, Strawbridge RJ, Halvorsen B, Yndestad A, Ranheim T, Krohg-Sorensen K, Skjelland M, Espvik T, Aukrust P. et al. NLRP3 inflammasome expression and activation in human atherosclerosis. *J Am Heart Assoc*. 2016;5:e003031. doi: 10.1161/JAHA.115.003031
  77. Mallat Z, Corbaz A, Scoazec A, Besnard S, Lesèche G, Chvatchko Y, Tedgui A. Expression of interleukin-18 in human atherosclerotic plaques and relation to plaque instability. *Circulation*. 2001;104:1598–1603.
  78. Rajamäki K, Lappalainen J, Oörni K, Välimäki E, Matikainen S, Kovanen PT, Eklund KK. Cholesterol crystals activate the NLRP3 inflammasome in human macrophages: a novel link between cholesterol metabolism and inflammation. *PLoS One*. 2010;5:e11765. doi: 10.1371/journal.pone.0011765
  79. Wu X, Zhang H, Qi W, Zhang Y, Li J, Li Z, Lin Y, Bai X, Liu X, Chen X. et al. Nicotine promotes atherosclerosis via ROS-NLRP3-mediated endothelial cell pyroptosis. *Cell Death Dis*. 2018;9:171.
  80. Mao C, Li D, Zhou E, Zhang J, Wang C, Xue C. Nicotine exacerbates atherosclerosis through a macrophage-mediated endothelial injury pathway. *Aging (Albany NY)*. 2021;13:7627–7643. doi: 10.18632/aging.202660
  81. Qian Z, Zhao Y, Wan C, Deng Y, Zhuang Y, Xu Y, Zhu Y, Lu S, Bao Z. Pyroptosis in the Initiation and Progression of Atherosclerosis. *Front Pharmacol*. 2021;12:652963. doi: 10.3389/fphar.2021.652963
  82. Schneider KS, Groß CJ, Dreier RF, Saller BS, Mishra R, Gorka O, Heilig R, Meunier E, Dick MS, Čiković T. et al. The inflammasome drives GSDMD-independent secondary pyroptosis and IL-1 release in the absence of caspase-1 protease activity. *Cell Rep*. 2017;21:3846–3859. doi: 10.1016/j.celrep.2017.12.018
  83. Speir M, Lawlor KE. RIP-roaring inflammation: RIPK1 and RIPK3 driven NLRP3 inflammasome activation and autoinflammatory disease. *Semin Cell Dev Biol*. 2021;109:114–124. doi: 10.1016/j.semcdb.2020.07.011

84. Lawlor KE, Khan N, Mildenhall A, Gerlic M, Croker BA, D'Cruz AA, Hall C, Kaur Spall S, Anderson H, Masters SL. et al. RIPK3 promotes cell death and NLRP3 inflammasome activation in the absence of MLKL. *Nat Commun*. 2015;6:6282. doi: 10.1038/ncomms7282
85. Tao L, Lin H, Wen J, Sun Q, Gao Y, Xu X, Wang J, Zhang J, Weng D. The kinase receptor-interacting protein 1 is required for inflammasome activation induced by endoplasmic reticulum stress. *Cell Death Dis*. 2018;9:641. doi: 10.1038/s41419-018-0694-7
86. Ridker PM, MacFadyen JG, Thuren T, Libby P. Residual inflammatory risk associated with interleukin-18 and interleukin-6 after successful interleukin-1beta inhibition with canakinumab: further rationale for the development of targeted anti-cytokine therapies for the treatment of atherothrombosis. *Eur Heart J*. 2019;41:2153–2163. doi: 10.1093/eurheartj/ehz542
87. Jiang M, Sun X, Liu S, Tang Y, Shi Y, Bai Y, Wang Y, Yang Q, Yang Q, Jiang W. et al. Caspase-11-Gasdermin D-mediated pyroptosis is involved in the pathogenesis of atherosclerosis. *Front Pharmacol*. 2021;12:657486. doi: 10.3389/fphar.2021.657486
88. Puylaert P, Van Praet M, Vaes F, Neutel CHG, Roth L, Guns P-J, De Meyer GRY, Martinet W. Gasdermin D deficiency limits the transition of atherosclerotic plaques to an inflammatory phenotype in ApoE knock-out mice. *Biomedicines*. 2022;10:1171.
89. Hu JJ, Liu X, Xia S, Zhang Z, Zhang Y, Zhao J, Ruan J, Luo X, Lou X, Bai Y. et al. FDA-approved disulfiram inhibits pyroptosis by blocking gasdermin D pore formation. *Nat Immunol*. 2020;21:736–745. doi: 10.1038/s41590-020-0669-6
90. Humphries F, Shmuel-Galia L, Ketelut-Carneiro N, Li S, Wang B, Nemmara VV, Wilson R, Jiang Z, Khalighinejad F, Muneeruddin K. et al. Succination inactivates gasdermin D and blocks pyroptosis. *Science*. 2020;369:1633–1637. doi: 10.1126/science.abb9818
91. Luo M, Sun Q, Zhao H, Tao J, Yan D. The effects of dimethyl fumarate on atherosclerosis in the apolipoprotein E-deficient mouse model with Streptozotocin-induced hyperglycemia mediated by the nuclear factor erythroid 2-related factor 2/antioxidant response element (nrf2/are) signaling pathway. *Med Sci Monit*. 2019;25:7966–7975. doi: 10.12659/msm.918951
92. Jiang K, Tu Z, Chen K, Xu Y, Chen F, Xu S, Shi T, Qian J, Shen L, Hwa J. et al. Gasdermin D inhibition confers antineutrophil-mediated cardioprotection in acute myocardial infarction. *J Clin Invest*. 2022;132:e151268. doi: 10.1172/jci151268
93. Rathkey JK, Zhao J, Liu Z, Chen Y, Yang J, Kondolf HC, Benson BL, Chirieleison SM, Huang AY, Dubyak GR. et al. Chemical disruption of the pyroptotic pore-forming protein gasdermin D inhibits inflammatory cell death and sepsis. *Sci Immunol*. 2018;3:eaat2738. doi: 10.1126/sciimmunol.aat2738
94. Rogers C, Fernandes-Alnemri T, Mayes L, Alnemri D, Cingolani G, Alnemri ES. Cleavage of DFNA5 by caspase-3 during apoptosis mediates progression to secondary necrotic/pyroptotic cell death. *Nat Commun*. 2017;8:14128. doi: 10.1038/ncomms14128
95. Schrijvers DM, De Meyer GR, Kockx MM, Herman AG, Martinet W. Phagocytosis of apoptotic cells by macrophages is impaired in atherosclerosis. *Arterioscler Thromb Vasc Biol*. 2005;25:1256–1261. doi: 10.1161/01.ATV.0000166517.18801.a7
96. Jarr KU, Nakamoto R, Doan BH, Kojima Y, Weissman IL, Advani RH, Igaru A, Leeper NJ. Effect of CD47 blockade on vascular inflammation. *N Engl J Med*. 2021;384:382–383. doi: 10.1056/NEJMc2029834
97. Martinet W, Knaapen MW, De Meyer GR, Herman AG, Kockx MM. Elevated levels of oxidative DNA damage and DNA repair enzymes in human atherosclerotic plaques. *Circulation*. 2002;106:927–932. doi: 10.1161/01.cir.0000026393.47805.21
98. Dolma S, Lessnick SL, Hahn WC, Stockwell BR. Identification of genotype-selective antitumor agents using synthetic lethal chemical screening in engineered human tumor cells. *Cancer Cell*. 2003;3:285–296. doi: 10.1016/s1535-6108(03)00050-3
99. Yagoda N, von Rechenberg M, Zaganjor E, Bauer AJ, Yang WS, Fridman DJ, Wolpaw AJ, Smukste I, Peltier JM, Boniface JJ. et al. RAS-RAF-MEK-dependent oxidative cell death involving voltage-dependent anion channels. *Nature*. 2007;447:864–868. doi: 10.1038/nature05859
100. Yang WS, Stockwell BR. Synthetic lethal screening identifies compounds activating iron-dependent, nonapoptotic cell death in oncogenic-RAS-harboring cancer cells. *Chem Biol*. 2008;15:234–245. doi: 10.1016/j.chembiol.2008.02.010
101. Harrison PM, Arosio P. The ferritins: molecular properties, iron storage function and cellular regulation. *Biochim Biophys Acta*. 1996;1275:161–203. doi: 10.1016/0005-2728(96)00022-9
102. Doll S, Freitas FP, Shah R, Aldrovandi M, da Silva MC, Ingold I, Goya Grocin A, Xavier da Silva TN, Panzilius E, Scheel CH. et al. FSP1 is a glutathione-independent ferroptosis suppressor. *Nature*. 2019;575:693–698. doi: 10.1038/s41586-019-1707-0
103. Bersuker K, Hendricks JM, Li Z, Magtanong L, Ford B, Tang PH, Roberts MA, Tong B, Maimone TJ, Zoncu R. et al. The CoQ oxidoreductase FSP1 acts parallel to GPX4 to inhibit ferroptosis. *Nature*. 2019;575:688–692. doi: 10.1038/s41586-019-1705-2
104. Yan HF, Zou T, Tuo QZ, Xu S, Li H, Belaidi AA, Lei P. Ferroptosis: mechanisms and links with diseases. *Signal Transduct Target Ther*. 2021;6:49. doi: 10.1038/s41392-020-00428-9
105. Papac-Milicevic N, Busch CJ, Binder CJ. Malondialdehyde epitopes as targets of immunity and the implications for atherosclerosis. *Adv Immunol*. 2016;131:1–59. doi: 10.1016/bs.ai.2016.02.001
106. Dixon SJ, Lemberg KM, Lamprecht MR, Skouta R, Zaitsev EM, Gleason CE, Patel DN, Bauer AJ, Cantley AM, Yang WS. et al. Ferroptosis: an iron-dependent form of nonapoptotic cell death. *Cell*. 2012;149:1060–1072. doi: 10.1016/j.cell.2012.03.042
107. Yang WS, SriRamaratnam R, Welsch ME, Shimada K, Skouta R, Viswanathan VS, Cheah JH, Clemons PA, Shamji AF, Clish CB. et al. Regulation of ferroptotic cancer cell death by GPX4. *Cell*. 2014;156:317–331. doi: 10.1016/j.cell.2013.12.010
108. Cao JY, Dixon SJ. Mechanisms of ferroptosis. *Cell Mol Life Sci*. 2016;73:2195–2209. doi: 10.1007/s00018-016-2194-1
109. Hassannia B, Vandenabeele P, Vanden Berghe T. Targeting ferroptosis to iron out cancer. *Cancer Cell*. 2019;35:830–849. doi: 10.1016/j.ccell.2019.04.002
110. Hassannia B, Wiernicki B, Ingold I, Qu F, Van Herck S, Tyurina YY, Bayir H, Abhari BA, Angeli JPF, Choi SM. et al. Nano-targeted induction of dual ferroptotic mechanisms eradicates high-risk neuroblastoma. *J Clin Invest*. 2018;128:3341–3355. doi: 10.1172/jci99032
111. Chang LC, Chiang SK, Chen SE, Yu YL, Chou RH, Chang WC. Heme oxygenase-1 mediates BAY 11-7085 induced ferroptosis. *Cancer Lett*. 2018;416:124–137. doi: 10.1016/j.canlet.2017.12.025
112. Youssef LA, Rebbaa A, Pampou S, Weisberg SP, Stockwell BR, Hod EA, Spitalnik SL. Increased erythrophagocytosis induces ferroptosis in red pulp macrophages in a mouse model of transfusion. *Blood*. 2018;131:2581–2593. doi: 10.1182/blood-2017-12-822619
113. Sullivan JL. Are menstruating women protected from heart disease because of, or in spite of, estrogen? relevance to the iron hypothesis. *Am Heart J*. 2003;145:190–194. doi: 10.1067/mhj.2003.142
114. de Valk B, Marx JJ. Iron, atherosclerosis, and ischemic heart disease. *Arch Intern Med*. 1999;159:1542–1548. doi: 10.1001/archinte.159.14.1542
115. Lee TS, Shiao MS, Pan CC, Chau LY. Iron-deficient diet reduces atherosclerotic lesions in apoE-deficient mice. *Circulation*. 1999;99:1222–1229. doi: 10.1161/01.cir.99.9.1222
116. Minqin R, Rajendran R, Pan N, Tan BK, Ong WY, Watt F, Halliwell B. The iron chelator desferrioxamine inhibits atherosclerotic lesion development and decreases lesion iron concentrations in the cholesterol-fed rabbit. *Free Radic Biol Med*. 2005;38:1206–1211. doi: 10.1016/j.freeradbiomed.2005.01.008
117. Zhang WJ, Wei H, Frei B. The iron chelator, desferrioxamine, reduces inflammation and atherosclerotic lesion development in experimental mice. *Exp Biol Med (Maywood)*. 2010;235:633–641. doi: 10.1258/ebm.2009.009229
118. Meyers DG, Jensen KC, Menitove JE. A historical cohort study of the effect of lowering body iron through blood donation on incident cardiac events. *Transfusion*. 2002;42:1135–1139. doi: 10.1046/j.1537-2995.2002.00186.x
119. Peffer K, den Heijer M, de Kort W, Verbeek ALM, Atsma F. Cardiovascular risk in 159 934 frequent blood donors while addressing the healthy donor effect. *Heart*. 2019;105:1260–1265. doi: 10.1136/heartjnl-2018-314138
120. Ponraj D, Makjanic J, Thong PS, Tan BK, Watt F. The onset of atherosclerotic lesion formation in hypercholesterolemic rabbits is delayed by iron depletion. *FEBS Lett*. 1999;459:218–222. doi: 10.1016/s0014-5793(99)01199-0
121. De Meyer GR, De Cleen DM, Cooper S, Knaapen MW, Jans DM, Martinet W, Herman AG, Bult H, Kockx MM. Platelet phagocytosis and processing of beta-amyloid precursor protein as a mechanism of macrophage activation in atherosclerosis. *Circ Res*. 2002;90:1197–1204. doi: 10.1161/01.res.0000020017.84398.61
122. Yuan XM, Li W, Baird SK, Carlsson M, Meleforts O. Secretion of ferritin by iron-laden macrophages and influence of lipoproteins. *Free Radic Res*. 2004;38:1133–1142. doi: 10.1080/10715760400011692
123. Meng Z, Liang H, Zhao J, Gao J, Liu C, Ma X, Liu J, Liang B, Jiao X, Cao J. et al. HMOX1 upregulation promotes ferroptosis in diabetic atherosclerosis. *Life Sci*. 2021;284:119935. doi: 10.1016/j.lfs.2021.119935
124. Friedmann Angeli JP, Schneider M, Proneth B, Tyurina YY, Tyurina VA, Hammond VJ, Herbach N, Aichler M, Walch A, Eggenhofer E. et

- al. Inactivation of the ferroptosis regulator Gpx4 triggers acute renal failure in mice. *Nat Cell Biol*. 2014;16:1180–1191. doi: 10.1038/ncb3064
125. Zilka O, Shah R, Li B, Friedmann Angeli JP, Griesser M, Conrad M, Pratt DA. On the Mechanism of Cytoprotection by Ferrostatin-1 and Liproxstatin-1 and the Role of Lipid Peroxidation in Ferroptotic Cell Death. *ACS Cent Sci*. 2017;3:232–243. doi: 10.1021/acscentsci.7b00028
  126. Skouta R, Dixon SJ, Wang J, Dunn DE, Orman M, Shimada K, Rosenberg PA, Lo DC, Weinberg JM, Linkermann A, et al. Ferrostatins inhibit oxidative lipid damage and cell death in diverse disease models. *J Am Chem Soc*. 2014;136:4551–4556. doi: 10.1021/ja411006a
  127. Bai T, Li M, Liu Y, Qiao Z, Wang Z. Inhibition of ferroptosis alleviates atherosclerosis through attenuating lipid peroxidation and endothelial dysfunction in mouse aortic endothelial cell. *Free Radic Biol Med*. 2020;160:92–102. doi: 10.1016/j.freeradbiomed.2020.07.026
  128. Guo Z, Ran Q, RobertsZhou L, Richardson A, Sharan C, Wu D, Yang H. Suppression of atherogenesis by overexpression of glutathione peroxidase-4 in apolipoprotein E-deficient mice. *Free Radic Biol Med*. 2008;44:343–352. doi: 10.1016/j.freeradbiomed.2007.09.009
  129. Bocan TM, Rosebury WS, Mueller SB, Kuchera S, Welch K, Daugherty A, Cornicelli JA. A specific 15-lipoxygenase inhibitor limits the progression and monocyte-macrophage enrichment of hypercholesterolemia-induced atherosclerosis in the rabbit. *Atherosclerosis*. 1998;136:203–216. doi: 10.1016/s0021-9150(97)00204-9
  130. Cyrus T, Witztum JL, Rader DJ, Tangirala R, Fazio S, Linton MF, Funk CD. Disruption of the 12/15-lipoxygenase gene diminishes atherosclerosis in apo E-deficient mice. *J Clin Invest*. 1999;103:1597–1604. doi: 10.1172/jci5897
  131. Hofmans S, Vanden Berghe T, Devisscher L, Hassannia B, Lyssens S, Joossens J, Van Der Veken P, Vandenabeele P, Augustyns K. Novel ferroptosis inhibitors with improved potency and ADME properties. *J Med Chem*. 2016;59:2041–2053. doi: 10.1021/acs.jmedchem.5b01641
  132. Devisscher L, Van Coillie S, Hofmans S, Van Rompaey D, Goossens K, Meul E, Maes L, De Winter H, Van Der Veken P, Vandenabeele P, et al. Discovery of Novel, drug-like ferroptosis inhibitors with in vivo efficacy. *J Med Chem*. 2018;61:10126–10140. doi: 10.1021/acs.jmedchem.8b01299
  133. Van Coillie S, Van San E, Goetschalckx I, Wiernicki B, Mukhopadhyay B, Tonnus W, Choi SM, Roelandt R, Dumitrascu C, Lamberts L, et al. Targeting ferroptosis protects against experimental (multi)organ dysfunction and death. *Nat Commun*. 2022;13:1046. doi: 10.1038/s41467-022-28718-6
  134. Perisic L, Hedin E, Razuvaev A, Lengquist M, Osterholm C, Folkersen L, Gillgren P, Paulsson-Berne G, Ponten F, Odeberg J, et al. Profiling of atherosclerotic lesions by gene and tissue microarrays reveals PCSK6 as a novel protease in unstable carotid atherosclerosis. *Arterioscler Thromb Vasc Biol*. 2013;33:2432–2443. doi: 10.1161/atvbaha.113.301743
  135. Arking DE, Juntila MJ, Goyette P, Huertas-Vazquez A, Eijgelsheim M, Blom MT, Newton-Cheh C, Reinier K, Teodorescu C, Uy-Evanado A, et al. Identification of a sudden cardiac death susceptibility locus at 2q24.2 through genome-wide association in European ancestry individuals. *PLoS Genet*. 2011;7:e1002158. doi: 10.1371/journal.pgen.1002158
  136. Ayari H, Bricca G. Identification of two genes potentially associated in iron-heme homeostasis in human carotid plaque using microarray analysis. *J Biosci*. 2013;38:311–315. doi: 10.1007/s12038-013-9310-2
  137. Zhou Y, Zhou H, Hua L, Hou C, Jia Q, Chen J, Zhang S, Wang Y, He S, Jia E. Verification of ferroptosis and pyroptosis and identification of PTGS2 as the hub gene in human coronary artery atherosclerosis. *Free Radic Biol Med*. 2021;171:55–68. doi: 10.1016/j.freeradbiomed.2021.05.009
  138. Burger F, Baptista D, Roth A, da Silva RF, Montecucco F, Mach F, Brandt KJ, Miteva K. NLRP3 Inflammasome activation controls vascular smooth muscle cells phenotypic switch in atherosclerosis. *Int J Mol Sci*. 2021;23: doi: 10.3390/ijms23010340
  139. Montecucco F, Lenglet S, Gayet-Ageron A, Bertolotto M, Pelli G, Palombo D, Pane B, Spinella G, Steffens S, Raffaghello L, et al. Systemic and intraplaque mediators of inflammation are increased in patients symptomatic for ischemic stroke. *Stroke*. 2010;41:1394–1404. doi: 10.1161/strokeaha.110.578369
  140. Li W, Xu LH, Forsell C, Sullivan JL, Yuan XM. Overexpression of transferrin receptor and ferritin related to clinical symptoms and destabilization of human carotid plaques. *Exp Biol Med (Maywood)*. 2008;233:818–826. doi: 10.3181/0711-rm-320
  141. Yuan XM. Apoptotic macrophage-derived foam cells of human atheromas are rich in iron and ferritin, suggesting iron-catalysed reactions to be involved in apoptosis. *Free Radic Res*. 1999;30:221–231. doi: 10.1080/10715769900300241
  142. Ijäs P, Nuotio K, Saksi J, Soinne L, Saimanen E, Karjalainen-Lindsberg ML, Salonen O, Sarna S, Tuimala J, Kovanen PT, et al. Microarray analysis reveals overexpression of CD163 and HO-1 in symptomatic carotid plaques. *Arterioscler Thromb Vasc Biol*. 2007;27:154–160. doi: 10.1161/01.ATV.0000251991.64617.e7
  143. Wu D, Hu Q, Wang Y, Jin M, Tao Z, Wan J. Identification of HMOX1 as a critical ferroptosis-related gene in atherosclerosis. *Front Cardiovasc Med*. 2022;9:833642. doi: 10.3389/fcvm.2022.833642
  144. Döring Y, Manthey HD, Drechsler M, Lievens D, Megens RT, Soehnlein O, Busch M, Manca M, Koenen RR, Pelisek J, et al. Autoantigenic protein-DNA complexes stimulate plasmacytoid dendritic cells to promote atherosclerosis. *Circulation*. 2012;125:1673–1683. doi: 10.1161/circulationaha.111.046755
  145. Finn AV, Nakano M, Polavarapu R, Karmali V, Saeed O, Zhao X, Yazdani S, Otsuka F, Davis T, Habib A, et al. Hemoglobin directs macrophage differentiation and prevents foam cell formation in human atherosclerotic plaques. *J Am Coll Cardiol*. 2012;59:166–177. doi: 10.1016/j.jacc.2011.10.852
  146. Tompson D, Whitaker M, Pan R, Johnson G, Fuller T, Zann V, McKenzie L, Abbott-Banner K, Hawkins S, Powell M. Development of a once-daily modified-release formulation for the short half-life RIPK1 inhibitor GSK2982772 using DiffCORE technology. *Pharm Res*. 2022;39:153–165. doi: 10.1007/s11095-021-03124-7
  147. Cohen DJ, Pant S, O'Neil B, Marini J, Winnberg J, Ahlers CM, Callaway J, Rathi C, Acosta A, Verticelli A, et al. A phase I/II study of GSK3145095 alone and in combination with anticancer agents including pembrolizumab in adults with selected solid tumors. *J Clin Oncol*. 2019;37:TPS4165–TPS4165. doi: 10.1200/JCO.2019.37.15\_suppl.TPS4165
  148. Vissers M, Heuberger J, Groeneveld GJ, Oude Nijhuis J, De Deyn PP, Hadi S, Harris J, Tsai RM, Cruz-Herranz A, Huang F, et al. Safety, pharmacokinetics and target engagement of novel RIPK1 inhibitor SAR443060 (DNL747) for neurodegenerative disorders: Randomized, placebo-controlled, double-blind phase I/II studies in healthy subjects and patients. *Clin Transl Sci*. 2022;15:2010–2023. doi: 10.1111/cts.13317
  149. Clot P-F, Farenc C, Suratt B, Krahnke T, Tardat A, Florian P, Pomponio R, Patel N, Wiekowski M, Lin Y, et al. Late breaking abstract - immunomodulatory and clinical effects of RIPK1 inhibitor SAR443122 in patients with severe COVID-19. *Eur Respir J*. 2021;58:PA2363. doi: 10.1183/13993003.congress-2021.PA2363
  150. <https://www.globenewswire.com/news-release/2021/10/06/2309876/0/en/Denali-Therapeutics-Announces-Positive-Clinical-Results-and-Regulatory-Progress-for-Development-Programs-in-Amyotrophic-Lateral-Sclerosis-ALS.html>. Accessed August 11, 2022.
  151. Ridker PM, Everett BM, Thuren T, MacFadyen JG, Chang WH, Ballantyne C, Fonseca F, Nicolau J, Koenig W, Anker SD, et al. Antiinflammatory Therapy with Canakinumab for Atherosclerotic Disease. *N Engl J Med*. 2017;377:1119–1131. doi: 10.1056/NEJMoa1707914
  152. Tardif JC, Kouz S, Waters DD, Bertrand OF, Diaz R, Maggioni AP, Pinto FJ, Ibrahim R, Gamra H, Kiwan GS, et al. Efficacy and safety of low-dose colchicine after myocardial infarction. *N Engl J Med*. 2019;381:2497–2505. doi: 10.1056/NEJMoa1912388
  153. Bouabdallaoui N, Tardif JC, Waters DD, Pinto FJ, Maggioni AP, Diaz R, Berry C, Koenig W, Lopez-Sendon J, Gamra H, et al. Time-to-treatment initiation of colchicine and cardiovascular outcomes after myocardial infarction in the Colchicine Cardiovascular Outcomes Trial (COLCOT). *Eur Heart J*. 2020;41:4092–4099. doi: 10.1093/eurheartj/ehaa659
  154. Nidorf SM, Eikelboom JW, Budgeon CA, Thompson PL. Low-dose colchicine for secondary prevention of cardiovascular disease. *J Am Coll Cardiol*. 2013;61:404–410. doi: 10.1016/j.jacc.2012.10.027
  155. Nidorf SM, Fiolet ATL, Mosterd A, Eikelboom JW, Schut A, Opstal TSJ, The SHK, Xu XF, Ireland MA, Lenderink T, et al. Colchicine in patients with chronic coronary disease. *N Engl J Med*. 2020;383:1838–1847. doi: 10.1056/NEJMoa2021372
  156. Shah B, Pillinger M, Zhong H, Cronstein B, Xia Y, Lorin JD, Smilowitz NR, Feit F, Rathnapala N, Keller NM, et al. Effects of Acute colchicine administration prior to percutaneous coronary intervention: COLCHICINE-PCI randomized trial. *Circ Cardiovasc Interv*. 2020;13:e008717. doi: 10.1161/circinterventions.119.008717
  157. Marchetti C, Swartzwelder B, Gamboni F, Neff CP, Richter K, Azam T, Carta S, Tengesdal I, Nemkov T, D'Alessandro A, et al. OLT1177, a  $\beta$ -sulfonyl nitrile compound, safe in humans, inhibits the NLRP3 inflammasome and reverses the metabolic cost of inflammation. *Proc Natl Acad Sci USA*. 2018;115:E1530–e1539. doi: 10.1073/pnas.1716095115
  158. Klück V, Jansen T, Janssen M, Comarniceanu A, Efdé M, Tengesdal IW, Schraa K, Cleophas MCP, Scribner CL, Skouras DB, et al. Dapansutril,

- an oral selective NLRP3 inflammasome inhibitor, for treatment of gout flares: an open-label, dose-adaptive, proof-of-concept, phase 2a trial. *Lancet Rheumatol.* 2020;2:e270–e280. doi: 10.1016/s2665-9913(20)30065-5
159. Wohlford GF, Van Tassel BW, Billingsley HE, Kadariya D, Canada JM, Carbone S, Mihalick VL, Bonaventura A, Vecchié A, Chiabrando JG. et al. Phase 1B, randomized, double-blinded, dose escalation, single-center, repeat dose safety and pharmacodynamics study of the oral NLRP3 inhibitor dapansutril in subjects with NYHA II-III systolic heart failure. *J Cardiovasc Pharmacol.* 2020;77:49–60. doi: 10.1097/fjc.0000000000000931
  160. <https://investors.vrtx.com/news-releases/news-release-details/vertex-announces-completion-phase-2-study-vx-765-people-epilepsy>. Accessed August 11, 2022.
  161. Tang D, Kang R, Berghe TV, Vandenabeele P, Kroemer G. The molecular machinery of regulated cell death. *Cell Res.* 2019;29:347–364. doi: 10.1038/s41422-019-0164-5
  162. Hu XM, Li ZX, Lin RH, Shan JQ, Yu QW, Wang RX, Liao LS, Yan WT, Wang Z, Shang L. et al. Guidelines for regulated cell death assays: a systematic summary, a categorical comparison, a prospective. *Front Cell Dev Biol.* 2021;9:634690. doi: 10.3389/fcell.2021.634690
  163. Uyy E, Suica VI, Boteanu RM, Cerveanu-Hogas A, Ivan L, Hansen R, Antohe F. Regulated cell death joins in atherosclerotic plaque silent progression. *Sci Rep.* 2022;12:2814. doi: 10.1038/s41598-022-06762-y
  164. Dodson M, Castro-Portuguez R, Zhang DD. NRF2 plays a critical role in mitigating lipid peroxidation and ferroptosis. *Redox Biol.* 2019;23:101107. doi: 10.1016/j.redox.2019.101107
  165. Wang B, Ge Z, Cheng Z, Zhao Z. Tanshinone IIA suppresses the progression of atherosclerosis by inhibiting the apoptosis of vascular smooth muscle cells and the proliferation and migration of macrophages induced by ox-LDL. *Biol Open.* 2017;6:489–495. doi: 10.1242/bio.024133
  166. He L, Liu YY, Wang K, Li C, Zhang W, Li ZZ, Huang XZ, Xiong Y. Tanshinone IIA protects human coronary artery endothelial cells from ferroptosis by activating the NRF2 pathway. *Biochem Biophys Res Commun.* 2021;575:1–7. doi: 10.1016/j.bbrc.2021.08.067
  167. Hu Q, Wei B, Wei L, Hua K, Yu X, Li H, Ji H. Sodium tanshinone IIA sulfonate ameliorates ischemia-induced myocardial inflammation and lipid accumulation in Beagle dogs through NLRP3 inflammasome. *Int J Cardiol.* 2015;196:183–192. doi: 10.1016/j.ijcard.2015.05.152
  168. Nikolettou V, Markaki M, Palikaras K, Tavernarakis N. Crosstalk between apoptosis, necrosis and autophagy. *Biochim Biophys Acta.* 2013;1833:3448–3459. doi: 10.1016/j.bbamcr.2013.06.001
  169. Lin Y, Devin A, Rodriguez Y, Liu ZG. Cleavage of the death domain kinase RIP by caspase-8 prompts TNF-induced apoptosis. *Genes Dev.* 1999;13:2514–2526. doi: 10.1101/gad.13.19.2514
  170. Ofengeim D, Yuan J. Regulation of RIP1 kinase signalling at the crossroads of inflammation and cell death. *Nat Rev Mol Cell Biol.* 2013;14:727–736. doi: 10.1038/nrm3683
  171. Chen KW, Demarco B, Heilig R, Shkarina K, Boettcher A, Farady CJ, Pelczar P, Broz P. Extrinsic and intrinsic apoptosis activate pannexin-1 to drive NLRP3 inflammasome assembly. *EMBO J.* 2019;38:e101368. doi: 10.15252/emboj.2019101638
  172. Zheng M, Kanneganti TD. The regulation of the ZBP1-NLRP3 inflammasome and its implications in pyroptosis, apoptosis, and necroptosis (PANoptosis). *Immunol Rev.* 2020;297:26–38. doi: 10.1111/imr.12909
  173. Chen L, Yin Z, Qin X, Zhu X, Chen X, Ding G, Sun D, Wu NN, Fei J, Bi Y. et al. CD74 Ablation rescues type 2 diabetes mellitus-induced cardiac remodeling and contractile dysfunction through pyroptosis-evoked regulation of ferroptosis. *Pharmacol Res.* 2022;176:106086. doi: 10.1016/j.phrs.2022.106086